Phase Separation in Polyelectrolyte Gels Interacting with Surfactants of Opposite Charge

Per Hansson,*,† Stefanie Schneider,‡ and Björn Lindman‡

Department of Physical Chemistry, Uppsala University, P.O. Box 532, S-75121 Uppsala, Sweden, and Physical Chemistry 1, Center for Chemistry and Chemical Engineering, Lund University, P.O. Box 124, S-22100 Lund, Sweden

Received: March 19, 2002; In Final Form: July 9, 2002

Macroscopic phase separation in covalent sodium polyacrylate (PA) networks following the absorption of cetyltrimethylammonium bromide/chloride (CTAB/C) from aqueous solutions is studied experimentally and theoretically. The gels are shown to consist of a solvent-swollen polyelectrolyte network (core), surrounded by a dense surface phase (skin) of polyion/surfactant complexes. The effect of core swelling on network structure and polyion/surfactant interaction in skins is discussed. It is demonstrated that the skin limits the swelling of the core. A model of the equilibrium swelling of phase separated gels is developed, taking into account the osmotic swelling of the core due to the presence of mobile counterions, the work of deformation of the core network, and the work of deformation of the skin. The last contribution is described using the theory of rubber elasticity. The core network is described using an empirical equation of state. The model is used to calculate the volume of gels after the absorption of various amounts of surfactant. Comparison with experiments shows that the agreement is satisfactory. The skin microstructure is investigated by means of small-angle X-ray scattering, optical birefringence, and time-resolved fluorescence quenching. The size, shape, and spatial organization of surfactant micelles is found to depend on the composition of the skin. Stoichiometric polyion/surfactant complexes (free from simple ions) form an ordered cubic structure (space group: *Pm*3*n*). The incorporation of bromide or chloride ions leads to a transition to hexagonal structure. The transition is related to the corresponding transition in complexes between linear PA and CTAB. Skins with cubic structure are found to be elastic and can be deformed at constant volume. The structural basis for the rubber-like behavior is discussed. The appearance of hexagonal skin microstructure is found to correlate with an anomalous swelling/deswelling pattern leading to the formation of "balloon gels".

Introduction

The interaction between polyions and surfactant micelles of opposite charge is strong. In fact, polyions induce surfactant self-assembly in very dilute solutions[1−13] by folding around micelles as depicted in Figure 1. In comparison with regular micellization involving counterion binding, the arrangement is favorable from an entropic viewpoint due to the release of 'condensed' counterions as polyions bind to the micelles.[14] This explains why the critical association concentration, cac, is lower than the cmc for the surfactant. The thermodynamics of surfactant self-assembly in polyelectrolyte solutions was addressed recently[15] by one of us, and has been studied using computer simulations by Wallin and Linse.[16−18] The interaction between polyions and oppositely charged colloids in general has attracted considerable interest,[19−24] in part due to possible applications to gene therapy.

The arrangement in Figure 1 has important consequences for the phase stability.[15,25−28] Due to the low net charge of the complex, the long-range osmotic repulsion between regular micelles is absent. Instead attractive bridging and electrostatic correlation forces are believed to be important, as demonstrated by Granfeldt at al.[25] using Monte Carlo simulations. The association of "polyion-dressed" micelles is cooperative since

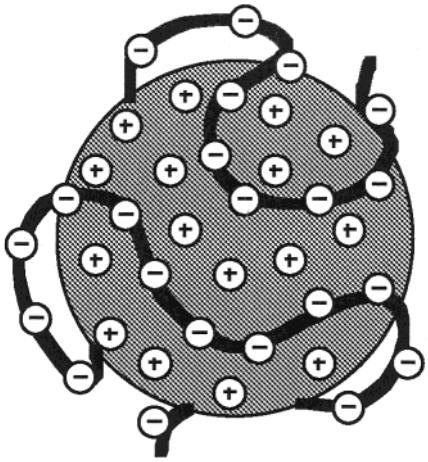

Figure 1. Schematic picture of a "polyion-dressed micelle",[15] the structural building block of polyion/surfactant complexes.

the number of favorable contacts between polyions and micelles increases with increasing cluster size. As a result, a polyelectrolyte/surfactant mixture tends to phase separate into a concentrated polyion/micelle phase ("coacervate") and a dilute solution phase.[14,29−31] This is illustrated in Figure 2a for stoichiometric mixtures. Depending on the conditions different structures appear in the concentrated phases, and the number of equilibrium phases may vary. A nonstoichiometric mixture phase separates in such a way that the excess of one of the

* Corresponding author. Present address: Department of Pharmacy, Biomedical Center, Uppsala University, P. O. Box 580, S-75123 Uppsala, Sweden. E-mail: Per.Hansson@farmaci.uu.se.

† Department of Physical Chemistry.

‡ Physical Chemistry 1.

10.1021/jp020745m CCC: $22.00
Published on Web 09/04/2002

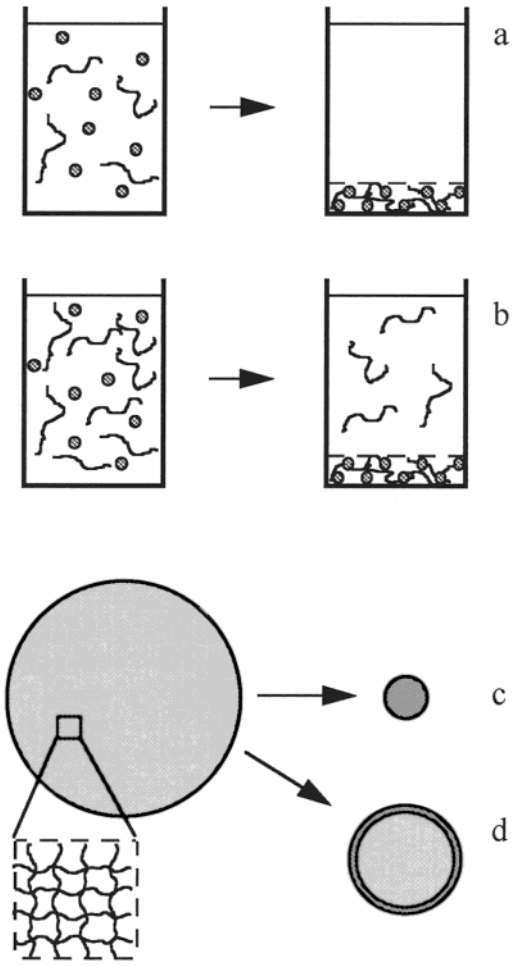

Figure 2. Phase separation in aqueous polyelectrolyte/surfactant systems. (a) Stoichiometric and (b) nonstoichiometric (excess of polyelectrolyte) mixtures of linear polyelectrolyte and surfactant. Volume transition of swollen gel absorbing (c) stoichiometric and (d) nonstoichiometric amounts of surfactant. Simple counterions are not shown.

components is left in the dilute phase, Figure 2b. Interestingly, similar events take place when cross-linked polyelectrolyte gels interact with oppositely charged surfactants. Swollen polyelectrolyte networks undergo a collapse after absorbing equimolar amounts of surfactant, as schematically depicted in Figure 2c. The volume transition is analogous to the process in Figure 2a. Likewise, when there is not enough surfactant available to form complexes involving all polyion chains in the network, the "excess" part of the network remains in a swollen state coexisting with the collapsed part. The collapsed part, containing the surfactant micelles, makes up a surface phase (skin) surrounding the water-swollen network (core), as illustrated in Figure 2d. This type of phase separation in gels was discovered by the group of Zezin and Kabanov,[32] and later but independently by Hansson.[33,34] The same phenomenon has been observed in gels absorbing proteins or short polyions of opposite charge to the network.[35,36] Quite different, however, from the case of fluid-fluid phase separation, the phases are chemically connected through the cross-links and constituents of a single macroscopic and elastic body.

It was pointed out by Panyukov and Rabbin,[37] working with transient surface phases in temperature sensitive gels, that the cross-links put constraints on the phase equilibrium not present in fluid systems. In the present paper we will explore one such aspect: namely, to what extent two phases coexisting in a

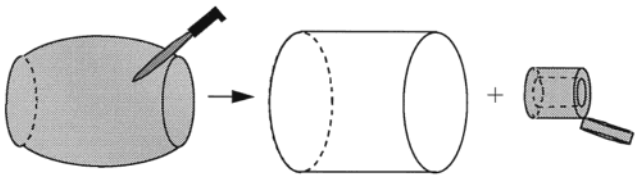

Figure 3. Illustration of the removal of skin from the core of a phase separated gel immersed in aqueous solution, and the subsequent contraction of skin and swelling of core.

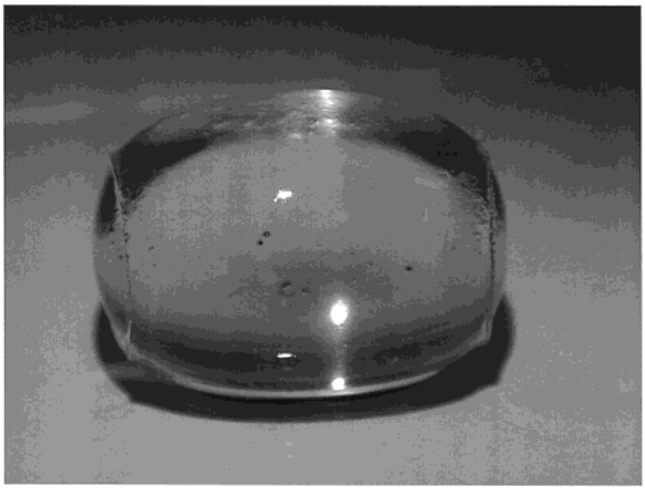

Figure 4. Photograph taken of an initially dry cylinder shaped PA gel (1% X) after absorbing water and CTA^+ from a CTAB solution (**II**). The shape of the phase separated gel ($\beta = 0.5$) is distorted due to the core swelling and the rubber elasticity of the skin. The skin can be removed from the core as shown in Figure 3.

network affect each other. A simple experiment described in Figure 3 points to the relevance of this problem. Shown to the left in the figure is a drawing of a phase separated gel obtained by letting a dry cylinder shaped sodium polyacrylate network (PA) swell in a solution of cetyltrimethylammonium bromide (CTAB). A picture of the gel, taken after incubation for one month, is shown in Figure 4. The gel in this state was cut as illustrated and the skin was physically separated from the swollen core. The surfactant-to-polyion molar ratio in the gel was 0.5. When placed back into the solution (containing about 2 mM of sodium bromide but only trace amounts of CTAB) the core was found to swell, and at the same time the skin contracted! The contraction was slow but significant and was accompanied by a thickening of the skin. However, the volume of the skin was essentially the same as before contraction. Interestingly, this resembles the elastic behavior of rubber. The interpretation is that the skin of the gel in Figure 4 acts as a (permeable) rubber membrane limiting the osmotic swelling of the core. The observation serves as background for the present investigations. The paper begins with a theoretical investigation of phase separation in covalent gels, where a model for the equilibrium swelling of PA gels in CTAB/C solutions is developed. The model considers, in particular, the effect of a dense surface phase on the swelling of the core. In the Results and Discussion part we first present theoretical results provided by the model, demonstrating the importance of elastic surface phases. Then follows experimental investigations of volume changes, composition, microstructure, and elastic behavior of skins and cores formed in PA/CTAB/C gels under various conditions. The structural basis for the rubber-like behavior of skins, and the structural transitions observed in them is discussed and compared with systems of linear polyions and surfactants

TABLE 1: Description of Investigated Systems

system	initial state of network	$C_{p,tot}$ (mM)	$C_{s,tot}$ (mM)	% X
I PA/CTAB	swollen	0.3−5	0.5	1
II PA/CTAB	dry	7	0−6	1
III PA/CTAC	swollen	4	0−5	1

of opposite charge. The paper ends with a comparison between model calculations and experimental data.

Materials and Methods

CTAB and CTAC from Serva and Cetylpyridinium chloride (C_{16}PC) from Merck were of analytic grade and used as supplied. Pyrene from Janssen (99%+), acrylic acid from Aldrich, *N*,*N*,*N*′,*N*′,-tetramethylethylenediamine (TEMED), ammonium persulfate, and *N*,*N*′-methylenebis(acrylamide) (MBA), all from Sigma, were used as received. Acrylic acid was polymerized for 12 h at 70 °C in the presence of 1, 1.5, and 3 mol % MBA as the cross-linking agent, using ammonium persulfate and TEMED as radical initiator and accelerator, respectively.[38] In the paper, the different degrees of cross linking will be referred to as 1% X, 1.5% X, and 3% X, respectively. The gels were neutralized in 0.5 M NaOH, cut into short cylinders and then repeatedly washed in 10^{-4} M NaOH. The polymer concentration in the pure network in equilibrium with 10^{-4} M NaOH was determined by weighing swollen and freeze-dried gels. The gels to be used for experiments were stored dry or swollen in 10^{-4} M NaOH. Gels were dried by slowly evaporating off water at ambient temperature. For this purpose a fan was used. The process transformed the gels into a compact glassy state.

Surfactant/gel samples were prepared by immersing dry or pre-swollen gel pieces in CTAB or CTAC solutions containing 10^{-4} M NaOH. Samples with different surfactant-to-polymer ratio were prepared either by varying the volume of the solution at fixed surfactant concentration or varying the total surfactant concentration at a fixed polymer concentration. After one month the concentration of surfactant in the solution was determined using a surfactant sensitive electrode as described elsewhere.[38] The result was used to calculate the degree of surfactant binding to the gels, β, defined as $\beta = n_s/n_p$, where n_s and n_p are the numbers of moles of surfactant and polyelectrolyte monomers, respectively, in the gel. The systems studied here are described in Table 1. In the text they will be referred to by roman numerals (**I**−**III**).

Fluorescence decays were recorded using the single photon counting technique as described in detail elsewhere.[7,33] Pyrene and CPC were used as fluorescent probe and quencher, respectively. Quenched decays were analyzed with the relationship:[39]

$$I(t) = I(0)\exp\{-t/\tau + \langle n\rangle(\exp\{-k_q t\} - 1)\} \qquad (1)$$

describing the time evolution of the fluorescence intensity $I(t)$ following a short laser pulse. $I(0)$ is the intensity at time zero, τ is the fluorescence lifetime in the absence of CPC, $\langle n\rangle$ is the average number of quencher per micelle, and k_q is the intramicellar quenching rate constant. Equation 1, which is a special case of the Infelta−Tachiya equation,[40,41] is valid when the probe and a randomly distributed quencher are stationary in the micelles during the probe lifetime. The average aggregation number N was calculated as $N = \langle n\rangle/X_Q$, where X_Q is the molefraction of quencher in the CP^+/CTA^+ mixed micelles. In all samples X_Q was assumed to be identical to the total molefraction of quencher in the system. This, as well as the assumption of a random distribution of quencher among the micelles, is an excellent approximation in the present system, as shown elsewhere.[33]

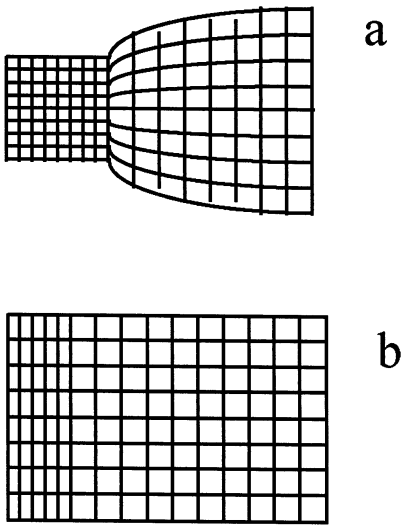

Figure 5. Schematic illustration of hypothetical states of phase separated networks. (a) Collapsed part isotropic, swollen part anisotropic. (b) Collapsed part anisotropic, swollen part isotropic.

Small-angle X-ray spectra were recorded using a linearly collimated Kratky compact small angle system equipped with a position sensitive detector (OED 50M from MBraun, Graz, Austria), as described elsewhere.[33]

When both TRFQ and SAXS were used the experiments were performed on the same gel specimens. All experiments in this study were carried out at 25 °C.

Theory

Preliminaries. In fluid systems the position of macroscopic phases relative to one another is determined by density. In gels gravity has little influence, instead the elasticity of the network plays a dominant role. A collapse of the network in one part of a gel will deform the network in other parts, as illustrated in Figure 5a. However, if the swollen network cannot be deformed a collapse in one direction may take place as shown in Figure 5b. Neither of the two cases is likely to represent an equilibrium situation unless the gels are very extended in one direction. Nevertheless, Figure 5b illustrates, schematically, a section of the border region between the swollen core and the dense surface phase in the gel shown in Figure 4. Thus, the network of a collapsed but intact surface phase is anisotropic or, to be precise, contracted in the direction perpendicular to the gel surface and extended laterally. (The lateral extension as a function of distance from the gel center must be continuous across the phase border[42]). The idea that will be pursued here is that the skin elasticity has a tendency to "restore" the network to its isotropic relaxed state. Conversely, the work needed to deform (stretch) the skin gives rise to a pressure in the core similar to the Laplace pressure in small droplets caused by surface tension (Figure 2d).

In liquid−liquid phase separation the interfacial tension acts as to decrease the contact area between the phases. In the present case it would favor a collapsed phase positioned in the center of the gel. However, that cannot be accomplished without a strong deformation of the network in the swollen part, similar to that shown in Figure 5a. For highly charged networks it is likely that the osmotic swelling pressure provided by the counterions forbids such an arrangement, and thus offers one

explanation to why the collapsed phase appears on the surface. It is likely, thus, that the position of the dense phase at the surface is the arrangement that gives rise to the smallest possible deformation of the swollen part of the network. (Another explanation would be that, since the surfactant enters the surface region first, the gel becomes "trapped" in a metastable state.)

Model. The purpose of the present treatment is to investigate how the presence of an anisotropic surface phase affects the swelling of the gel core. Consider a phase separated gel, i.e., a swollen core surrounded by a dense skin as depicted in Figure 2d. The gel, which is assumed to be spherical, is immersed in an aqueous solution. The gel contains a fixed number of moles n_p of polymer units (here acrylate groups), a fraction β' of them which are found in the skin. (For a list a symbols, see end of paper.) The density of network chains is assumed to be uniform (but, in general, not the same) in the core and the skin. Thus, the average swelling of the network can be described by v_{core} and v_{skin}, the volume of core and skin, respectively, per mole of polymer units. The gel volume is then given by

$$V = V_{core} + V_{skin} \tag{2}$$

where

$$V_{core} = n_p(1 - \beta')v_{core} \tag{3}$$

and

$$V_{skin} = n_p\beta' v_{skin} \tag{4}$$

With a volume $V_0 = n_p v_0$ of the surfactant-free gel ($\beta' = 0$), one obtains

$$\frac{V}{V_0} = \frac{v_{core}}{v_0} - \left(\frac{v_{core} - v_{skin}}{v_0}\right)\beta' \tag{5}$$

Before continuing we note that for non-crosslinked systems the composition of two phases in equilibrium does not depend on the amounts of them present. If that would apply here, v_{skin} and v_{core} would be constants and the latter equal to v_0 (at a fixed osmotic pressure). Then, since $v_{skin} \ll v_{core}$:

$$\frac{V}{V_0} \approx 1 - \beta' \tag{6}$$

Equations 5 and 6 were previously used to model the swelling of PA/DoTAB gels.[38] However, as can be inferred from previous sections, v_{core} is not constant but decreases as β' increases, i.e., as more skin is formed.

The work required to maintain the skin in its stretched-out state gives a contribution to the osmotic pressure in the gel core, which we denote π_{skin}. To derive an expression for π_{skin} we model the skin as a perfect rubber with v_{skin} constant. (The validity of this will be discussed below.) For simplicity we restrict ourselves to spherical gels. Then, if γ is the work (per unit area) of increasing the surface area of the skin, the resulting pressure can be calculated from the "Laplace equation":

$$\pi_{skin} - \frac{2\gamma}{R} \tag{7}$$

where R is the radius of the core. Thus, γ is considered as a "surface tension". The negative sign in (7) comes from the fact that the osmotic pressure (in the core) decreases as the pressure increases. According to the theory of rubber elasticity (see, e.g., Treloar[43]) the work of stretching a flat sheet of rubber by equal amounts in two directions at right angles is (per unit area):

$$\gamma = \frac{nRT}{A_{ref}}\left(1 - \left(\frac{A_{ref}}{A}\right)^3\right) \tag{8}$$

where n is the number of moles of polymer chains in the sheet, A_{ref} is the surface area of the sheet in its relaxed reference state, and A the area in the extended state. R is the ideal gas constant, and T is the absolute temperature. Since our intention is, mainly, to demonstrate the importance of the skin elasticity, we shall neglect the fact that the skin is curved and use (8) in (7) to calculate π_{skin}. This is expected to be a good approximation as long as the skin is thin compared with the gel radius. Indeed, by using the radius of the core for R in (7) the skin is assumed to be infinitely thin.

According to the theory behind (8) the network is in its reference state when all the chains are relaxed, which means that the network is isotropic. However, when the network in the skin is isotropic, the average degree of swelling is the same everywhere in the gel, i.e., $v_{skin} = v_{core}$. This follows from the fact that the core network is isotropic of symmetry reasons. Thus, to express π_{skin} in a useful form we first note that

$$\left(\frac{A_{ref}}{A}\right)^3 = \left(\frac{v_{core,ref}}{v_{core}}\right)^2 = \left(\frac{v_{skin}}{v_{core}}\right)^2 \tag{9}$$

where $v_{core,ref}$ ($=v_{skin}$) is the volume per moles of polymer units in the core when the skin is in its reference state. Then, since $R = 3V_{core}/A$ and $n = n_p\beta'/p$, where p is the average number of polymer units between consecutive cross-links, (3) and (7)–(9) can be combined to give:

$$\pi_{skin} = -\frac{\beta'}{1 - \beta'}\frac{2RT}{3p(v_{skin})^{2/3}(v_{core})^{1/3}}\left(1 - \left(\frac{v_{skin}}{v_{core}}\right)^2\right) \tag{10}$$

To find the equilibrium swelling of the gel we need to add to π_{skin} the other contributions to the osmotic pressure. The condition for swelling equilibrium can be written:

$$\Delta\pi_{ion} + \pi_{net} + \pi_{skin} = 0 \tag{11}$$

where $\Delta\pi_{ion}$ is the swelling pressure due to the difference in activity of mobile ions in the gel and in the surrounding solution. For highly charged ionic gels, the swelling pressure due to mixing of solvent with polymer chains is very small compared with $\Delta\pi_{ion}$ and can be neglected. π_{net} is due to the elastic response of the network chains as they are deformed from their relaxed reference state. For highly charged chains, with non-Gaussian distribution of end-to-end distances, this contribution is difficult to calculate theoretically.[44] Here, an empirical relationship will be used (see below).

Equation 11 expresses the equilibrium requirement that the chemical potential of water is the same in the gel and in the solution. Note that positive contributions to the osmotic pressure in the core promote swelling. In the absence of skin, e.g., in a surfactant-free system, swelling equilibrium is at hand when $\Delta\pi_{ion}$ is exactly balanced by π_{net}. When a skin is formed π_{skin} adds to the overall osmotic pressure in the core.

To estimate $\Delta\pi_{ion}$ we will assume that the activity of mobile ions in the gel core is the same as in an equally concentrated solution of linear sodium polyacrylate. The osmotic pressure in the latter is reasonably well described by the cylindrical Poisson–Boltzmann (PB) cell-model. The results from PB-calculations (see Appendix) give that $\Delta\pi_{ion}$ as a function of

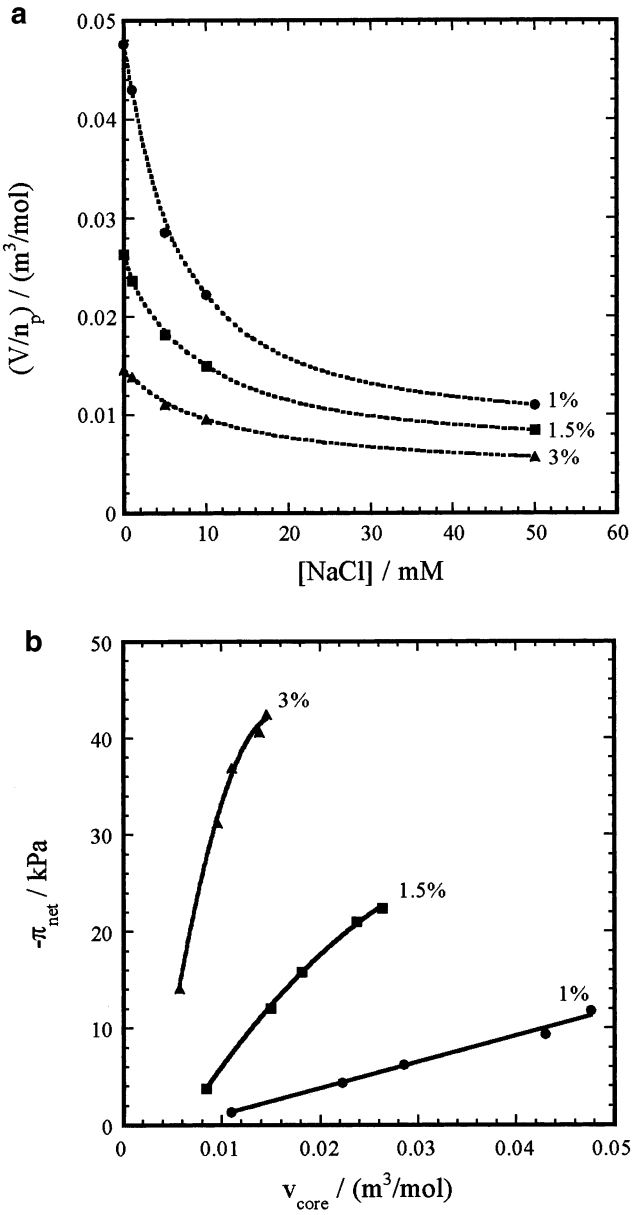

Figure 6. Equilibrium swelling of PA gels with 1, 1.5, and 3% X in bulk NaCl solutions. (a) Volume per moles of polyelectrolyte units in gels (V/n_p) plotted vs the concentration of NaCl in the solution. Dotted lines are just guides to the eye. (b) "Equations of state" for PA networks; $-\pi_{net}$ as a function of v_{core}, obtained from the data in Figure 6a as described in the text. Lines show (13) with the parameters in Table 1.

v_{core} can be described by relationships of the form:

$$\Delta\pi_{ion} = k_1 + \frac{k_2}{v_{core}} + \frac{k_3}{(v_{core})^2} \qquad (12)$$

where $k_1 - k_3$ are constants that have different values depending on the concentration of 1:1 electrolyte in the solution (C_{salt}).

π_{net} will be extracted from the data in Figure 6a showing V/n_p as a function of NaCl concentration in surfactant-free solutions. (Note that $V/n_p = v_{core}$ when $\beta = 0$.) The results for gels with 1, 1.5, and 3% X are shown. Since there is no skin present π_{net} must be equal to $-\Delta\pi_{ion}$ for each v_{core}. By calculating $\Delta\pi_{ion}$ as described above one can construct an "equation of state" for the network by plotting π_{net} versus v_{core}. The result, given in Figure 6b, shows that $-\pi_{net}$ increases approximately linearly with v_{core} in the range investigated. The

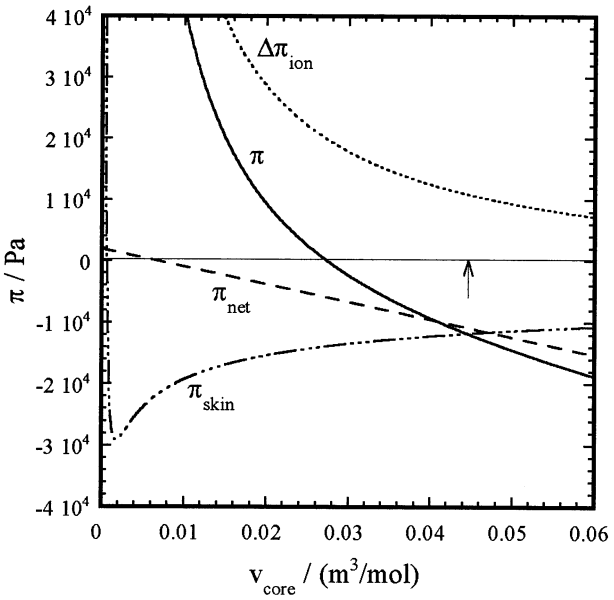

Figure 7. Total osmotic pressure p and the contributions from $\Delta\pi_{ion}$, π_{net}, and π_{skin} as a function of v_{core}, calculated for a gel with $\beta' = 0.5$, $p = 50$, and $v_{skin} = 7 \times 10^{-4}$ m^3/mol in 0.4 mM 1:1-electrolyte solution. Arrow: v_{core} corresponding to swelling equilibrium in the absence of skin ($\Delta\pi_{ion} = -\pi_{net}$). $T = 298$ K.

TABLE 2: Parameters Describing π_{Net} as a Function of v_{Core}

% X	k_4/Pa	k_5/(Pa mol/m^3)	k_6/(Pa(mol/m^3)^2)
1	1.70×10^3	-2.73×10^5	0
1.5	1.01×10^4	-1.83×10^6	2.21×10^7
3	2.73×10^4	-8.84×10^6	2.81×10^8

data can be fitted to a second-order polynom to give a (semi-) empirical relation between π_{net} and v_{core}:

$$\pi_{net} = k_4 + k_5 v_{core} + k_6 (v_{core})^2 \qquad (13)$$

where $k_4 - k_6$ are constants for a given network; see Table 2.

Results and Discussion

Theoretical Results. In this section we combine the above relations to show how the swelling of the core is affected by the skin according to the model. Figure 7 illustrates the swelling equilibrium for a 1% X PA gel with $\beta' = 0.5$, in contact with a 0.4 mM solution of a 1:1 electrolyte. The figure gives the total osmotic pressure (π) as a function of v_{core} as well as the individual contributions $\Delta\pi_{ion}$, π_{net}, and π_{skin}. v_{skin} is equal to 7×10^{-4} m^3/mol. The equilibrium situation corresponds to $\pi = 0$. As can be seen, the swelling of the core is substantially lower than that in the absence of skin. The swelling of the network in the absence of skin, indicated by an arrow in the figure, is obtained when $\Delta\pi_{ion} = -\pi_{net}$.

At the point where the π_{skin} curve intersects the x-axis the skin is in its reference state (i.e., $v_{core} = v_{skin}$). Any deviation from this gives rise to a restoring force in the skin, contributing to the osmotic pressure in the core. In practice, positive pressures from the skin are not encountered since, in general, $v_{core} \gg v_{skin}$. For small values of v_{core}, π_{skin} decreases as a function of v_{core} because the tension increases as the skin is stretched. Very soon, however, the tension reaches a constant value; see (8). The minimum in the π_{skin} curve arises because, at constant tension, the osmotic pressure decreases in magnitude (becomes less negative) as the volume of the core increases; see (7). This is of the same reason as the Laplace pressure is smaller in a large

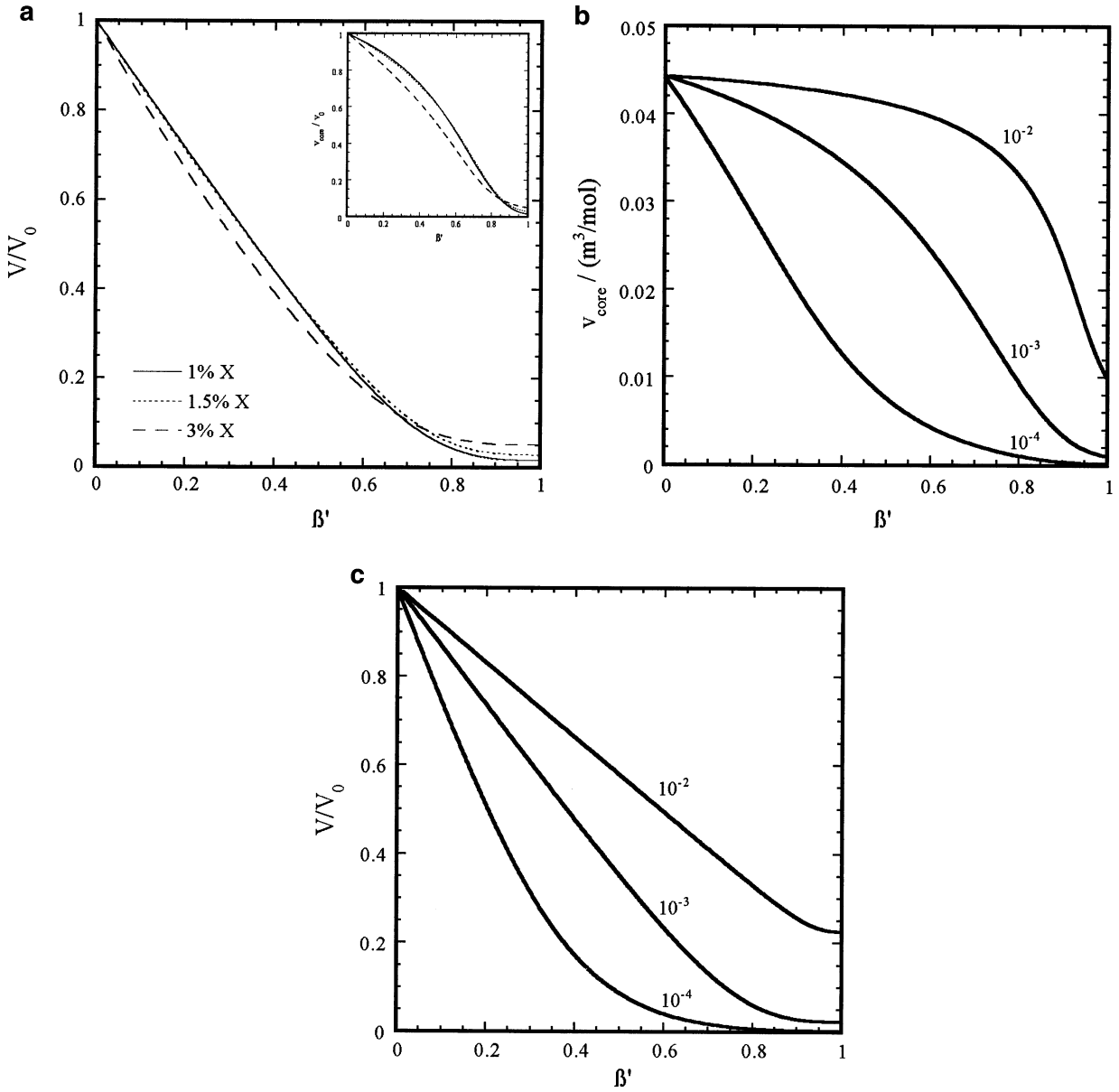

Figure 8. Model calculations for PA gels in 0.4 mM 1:1 electrolyte solutions. $T = 298$ K. (a) V/V_0 vs β' for gels with 1, 1.5, and 3% X ($p = 50$, 33, and 11, respectively); $\upsilon_{skin}=7 \times 10^{-4}$ m^3/mol. Inset shows $\upsilon_{core}/\upsilon_0$ vs β' for the same systems. (b) v_{core} vs β' for gels with 1% X ($p = 50$); $\upsilon_{skin} = 10^{-2}$, 10^{-3}, and 10^{-4} m^3/mol (indicated). (c) V/V_0 vs β' for gels with 1% X; $\upsilon_{skin} = 10^{-2}$, 10^{-3}, and 10^{-4} m^3/mol (indicated).

bubble than in a small one. In fact, the behavior of the π_{skin} curve is in agreement with the experience of inflating a balloon: initially a large pressure must be applied, but as a the size increases above a "critical" value it becomes easier.

It is noticeable that the total osmotic pressure decreases monotonically as v_{core} increases, and equals zero for a unique degree of swelling. It shows that the core should not become "trapped" in a nonequilibrium state, and that a gel has only one mechanical equilibrium state.

Naturally, by increasing β' the effect of the skin becomes larger. This leads to a smaller equilibrium swelling of the core. Figure 8a shows how $\upsilon_{core}/\upsilon_0$ (inset) and V/V_0 depend on β' when $\upsilon_{skin}=7 \times 10^{-4}$ m^3/mol and the gels are in equilibrium with a 0.4 mM solution of a 1:1 electrolyte. The curves have been obtained by inserting (10), (12), and (13) in (11) and solving for β'. V/V_0 was obtained by inserting υ_{core} into (5). It is clear that the skin has a strong effect on the swelling of the core. At the particular salt concentration considered here, υ_{core} decreases by a factor of 67, 35, and 20 for gels with 1, 1.5, and 3% X, respectively, as β' increases from zero to unity.

Importantly, V/V_0 is found to decrease rapidly with β' unitil $\beta' \approx 0.8$ where it levels out. At this point the core network is rather compressed, and so the conversion of core to skin does not lead to a strong volume change. It should be mentioned that the similarity between V/V_0-curves for gels with different degrees of cross-linking is in agreement with experiments.[34,38]

All results presented so far have been obtained with $\upsilon_{skin} = 7 \times 10^{-4}$ m^3/mol, a value typical for PA/CTAB skins with $\beta > 0.5$ (see below). It also equals the volume per poly(acrylic acid) unit in the network before neutralization with NaOH and swelling in water. The importance of this parameter is illustrated in Figure 8b where υ_{core} is plotted against β' with υ_{skin} equal to 10^{-4}, 10^{-3}, and 10^{-2} m^3/mol, respectively. The calculations have been made for 1% X gels in 0.4 mM electrolyte solution. The corresponding V/V_0 curves are shown in Figure 8c.

Before closing this section we note that, when normalized by υ_0, the υ_{core} curves for the gels with 1 and 1.5% X nearly

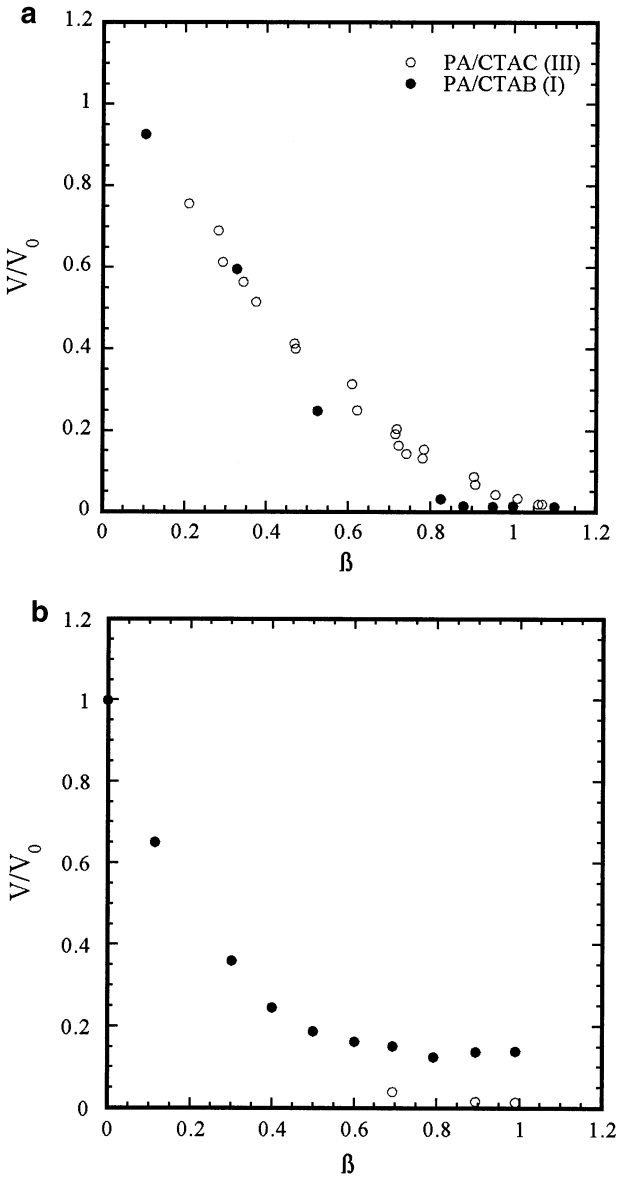

Figure 9. Experimental estimates of V/V_0 vs β for 1% X PA gels in CTAB/C solutions containing 10^{-4} M NaOH. (a) Shrinking of pre-swollen gels in 0.50 mM CTAB at different total concentration of PA (**I**), and in CTAC solutions of different concentrations ($C_{p,tot} = 4$ mM) (**III**). (b) Swelling of dry gels in CTAB solutions of different concentrations ($C_{p,tot} = 7$ mM) (**II**). Open symbols (b): V/V_0 for balloon gels with volume of enclosed liquid subtracted (see text).

overlap (see Figure 8a inset), and the one for 3% X deviates only little from the other two. Furthermore, the shapes of the curves suggest the approximation $v_{core}/v_0 \approx 1 - \beta'$ to be made. By inserting this expression into (5) one obtains

$$\frac{V}{V_0} \approx (1-\beta')^2 - \frac{v_{skin}}{v_0}\beta' \approx (1-\beta')^2 \qquad (14)$$

where the last approximation is valid when $v_{skin} \ll v_0$, as is the case for the gels with 1 and 1.5% cross-linker (see below). The function $V/V_0 = (1-\beta')^2$ may be a useful approximation when a closed form expression is needed.

Gel Volume. Experimentally determined volumes of 1% X PA networks immersed in CTAB and CTAC solutions are presented in Figure 9; see Table 1 for details about the systems investigated. Figure 9a shows how the volume of pre-swollen gels (**I**,**III**) decreases as a function of β, the amount of surfactant

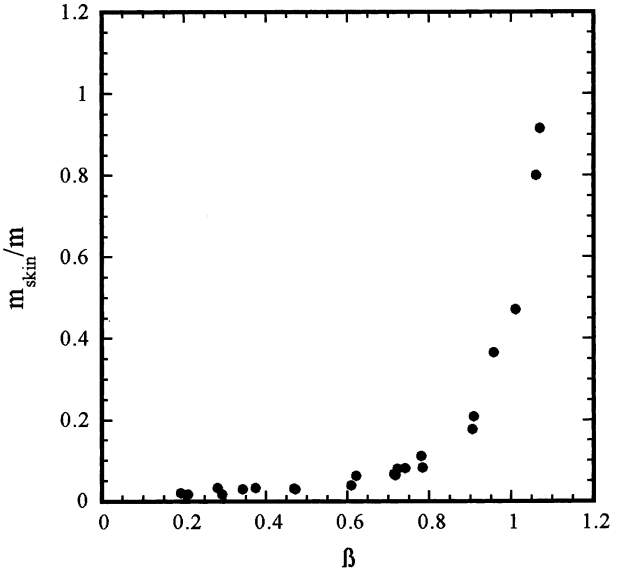

Figure 10. Weight fraction of skin (m_{skin}/m) in PA/CTAC gels (**III**) plotted vs β.

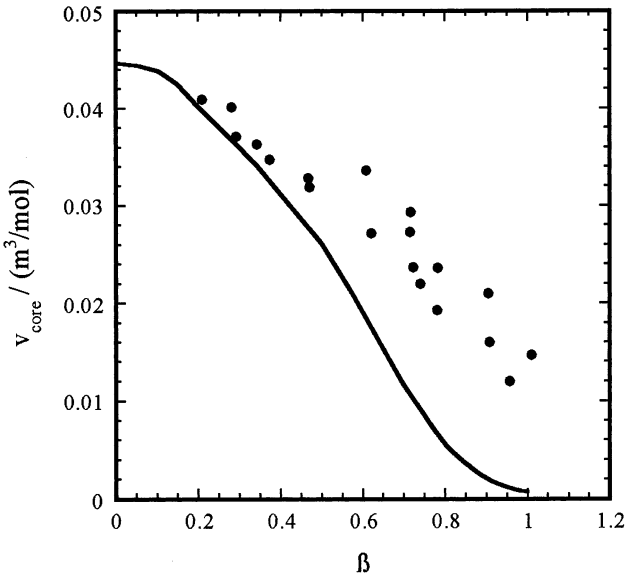

Figure 11. Volume of gel core (v_{core}) of PA/CTAC gels plotted vs β. Symbols: experimental data from system **III**. Line: model calculations (see text).

absorbed per polyion charged group. V_0 is the gel volume in 10^{-4} M NaOH aqueous solutions free from surfactant. As can be seen, CTAB and CTAC gave similar effects, indicating that the specific nature of the counterion is of secondary importance.

The binding of surfactant leads to a decrease of the gel core and an increase of the skin volume. This describes the progressive collapse of the network taking place at the interface between the swollen core and the dense surface phase. At sufficiently large β the entire network appears to be converted to a collapsed state. The volume of gels in this state is much smaller than V_0, showing that the skin contribution to the volume of the gels is small and important only at large β. This is evident from Figure 10 where the mass fraction (≈volume fraction) of skin in PA/CTAC gels (**III**) is plotted against β.

The effect of the skin on the core swelling is shown in Figure 11 where v_{core} for PA/CTAC gels (**III**) is plotted against β (symbols). The result is of great conceptual importance since it provides direct evidence that the swelling of the core network,

not only the amount of polymer in it, decreases as the amount of polymer in the skin increases. Thus, distinct from the case of liquid/liquid-phase equilibrium, the *composition* of one phase depends on the *volume* of the other phase.

As mentioned in the Introduction, occasionally, at high β, the gels have been transformed into a skin enclosing a liquid solution, sometimes containing small core fragments.[33,34] These "balloon gels", which will be discussed in more detail below, also appear when dried PA networks swell in surfactant solution (**II**). The volume progression for such gels is shown in Figure 9b. For comparison both the total volume of gel pieces (normalized by V_0) and the gel volume minus the volume of the encapsulated liquid are shown. The latter data resembles the behavior of PA gels shrinking in CTAB solutions (**I**) shown in Figure 9a, but V/V_0 decreases stronger with increasing β in the entire range. The difference can be attributed to different experimental conditions: while in system **I** the osmotic pressure in the surrounding aqueous solution is fixed, it increases with β in system **II** (see below).

Distribution of Surfactant. Water and mobile ions (including the surfactant) distribute between three regions: aqueous solution, gel core, and skin. Binding isotherms describing the partitioning of CTAB between solution and PA gels were presented in a preliminary report.[34] The same type of measurements were carried out here for PA/CTAC (**III**) and used to calculate β in Figure 9. The amount of free surfactant was found to be negligibly small compared with that in the gel.

The distribution of surfactant between skin and core was determined indirectly by monitoring the partitioning of a hydrophobic fluorophore (pyrene) between the two phases. For all samples the fluorescence signal from the skin was very strong. In contrast, hardly any fluorescence could be detected from the core, proving that only trace amounts ($<10^{-7}$ M) of the probe were present. This revealed that the latter contained no, or very few, surfactant micelles. The concentration of unimers should also be negligible since the cac in the gels is very low. The cac for DoTAB was previously[38] found to be 2×10^{-4} M in 1% X PA gels, and that of CTAB/C is expected to be about 2 orders of magnitude lower.[11] Thus we conclude that essentially all surfactant is located in the skin.

Composition of Skin. In this section we present a rather detailed investigation of the composition of skins. The information obtained is useful when comparing experimental volume data and theoretical calculations. In Figure 12a the weight percentage of water (wt % H_2O) in skins from PA/CTAC gels (**III**) is given. The results were obtained by weighing skins before and after vacuum-drying. As can be seen, the skins formed at low β contained substantial amounts of water, but the water content decreased with increasing β.

In Figure 13 we have plotted the skin thickness for PA/CTAC gels (**III**) obtained in two different ways. Filled symbols represent direct measurements with a micrometer. Open symbols were obtained from the ratio of the skin surface area to the skin volume. The area was calculated from diameter and length, and the volume calculated from the mass of the skin using a density equal to that of water. Note that the skin is very thin at low β. The satisfactory agreement between the two types of estimate in Figure 13 indicates that the density of skins used in the calculations is correct (1.0 g/mL). This is further supported by the observation that some of the gels with high β sink very slowly in the solution, and some even float. Of course, for skins with high water content there is no reason to believe the density to be different from that of water. A density equal 1.0 g/mL was reported earlier[33] for fully collapsed PA/DoTAB gels.

With the density known, the concentration of surfactant in skins can be calculated directly from the mass of skins and the number of moles of bound surfactant. In Figure 12b we have plotted the inverse of the surfactant concentration, i.e., V_{skin}/n_s, as a function of β. Again the result indicates that the skins formed at low β are more water swollen than at higher β, in agreement with the results in Figure 12a. Note that, the estimates in Figure 12a,b, respectively, are based on different types of measurements and thus represent independent estimates. Importantly, however, they can be combined to give the apparent molar mass (M_{app}) of the surfactant/polyion complexes in the skin. By defining the latter quantity as the dry weight of skin divided by n_s, we can write:

$$\frac{\text{wt \% } H_2O}{100} = 1 - \frac{M_{app} n_s}{m_{skin}} \tag{15}$$

where m_{skin} is the mass of wet skin. In Figure 12c (1 − wt % H_2O/100) is plotted vs n_s/m_{skin}. From the slope of the straight line fitted to the data we obtain $M_{app} = 355.4$ g/mol. This is very close to the (monomer) molar mass of CTAPA (=355.7 g/mol), suggesting that complexes in the skins are stoichiometric. Strictly, this conclusion can be made only if there is no simple salt (i.e., NaCl) in the skin contributing to M_{app}. However, with the electroneutrality of the skins as the only constraint, the following general relationship can be derived:

$$\frac{M_{app}}{M_{NaCl}} - \frac{M_{CTAC}}{M_{NaCl}} + \frac{1 - M_{NaPA}/M_{NaCl}}{\beta_{skin}} = \frac{n_{Na}}{n_{CTA}} \geq 0 \tag{16}$$

where n_{Na} and n_{CTA} are the number of moles of Na^+ and CTA^+ ions, respectively, in the skin, M_i is the molar mass of electrolyte i, and β_{skin} is the molar ratio of surfactant to polyion in the skin. Note, β_{skin} is an important quantity that will be used to relate β' to β in the last paragraph of the paper. With the value of M_{app} obtained from Figure 12c it follows immediately from (16) that $\beta_{skin} \geq 1.01$. By taking into account also the error in the estimate of M_{app} one obtains that $\beta_{skin} \geq 0.95$. The latter was calculated by taking 357.6 g/mol as an upper limit of M_{app}, as suggested by the standard error from the fit; see Figure 12c inset. This is the best estimate we can obtain without any assumptions regarding the distribution of neutral salt. However, due to the Donnan effect[45] only very small amounts of NaCl should be present in the skins once β_{skin} deviates from unity. (Remember that the concentrations of surfactant and polyion in the skins are very high.) This leads to the simplification that n_{Na}/n_{CTA} equals zero when surfactant is in excess ($\beta_{skin} > 1$), and $(1 - \beta_{skin})/\beta_{skin}$ when the polyion is in excess ($\beta_{skin} < 1$). By considering the standard error in the estimate of M_{app} we obtain $0.97 < \beta_{skin} < 1.08$. The conclusion is that the skins contain nearly equal amounts of polyion and surfactant, or a small excess of the latter.

Bromide Ions in PA/CTAB Skins. The estimated value of β_{skin} in the previous section was obtained for PA/CTAC gels (**III**) with β in the range from zero to unity. If $\beta_{skin} > 1$ there must be surfactant counterions in the skins to make them electroneutral. For PA/CTAB it is possible to detect the presence of bromide ions in the skins using a spectroscopic method, which in turn gives information about β_{skin} and how it depends on β.

Since bromide ions are quenchers of pyrene fluorescence the binding to micelles reduces the fluorescence lifetime, τ, of the probe dissolved in the micelles. The result from lifetime measurements on PA/CTAB (**I**) skins is shown in Figure 14, where τ is plotted against β (symbols). The lifetime is long and

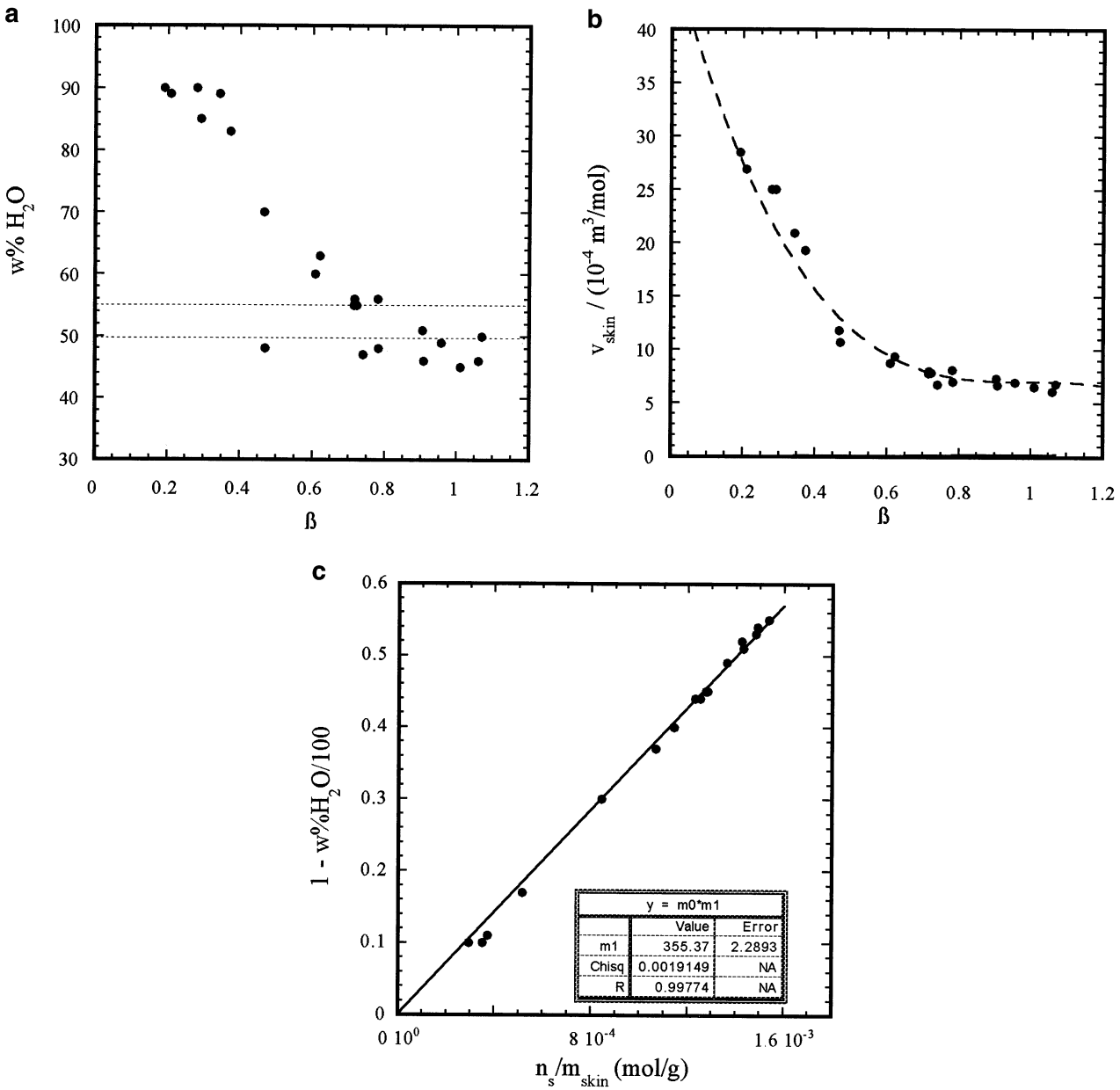

Figure 12. (a) Weight percentage of water in skins (wt % H_2O) plotted vs β for PA/CTAC gels (**III**). Dotted lines: extension of the cubic phase for linear CTAPA/H_2O[28] (see text). (b) Volume per moles of surfactant in skins (v_{skin}) of PA/CTAC gels (**III**) plotted vs β. Dashed line: mathematical function fitted to the experimental data, used in calculations presented in Figure 19b,c (see text). (c) Determination of apparent molar mass (M_{app}) for complexes in skins of PA/CTAC gels (**III**). 1 − wt % H_2O/100 is plotted vs n_s/m_{skin}. Symbols: experimental data. Line: linear fit passing through origin, with slope (inset) equal to M_{app}; see (15).

nearly constant for β values up to about 0.8. At higher β quenching is observed, revealing that bromide ions bind to the micelles. The data can be analyzed by considering that $1/\tau$ is a sum of three decay rates:[7]

$$\frac{1}{\tau} = k_0 + k_{ox}[O_2] + k_{Br}\theta \tag{17}$$

where k_0 is the natural decay rate, k_{ox} is the second-order rate constant for quenching by oxygen, and $[O_2]$ is the concentration of oxygen in water. k_{Br} is the pseudo first-order rate constant for quenching by bromide ions, and θ is the number of bound bromide ions per micelle charge. Equation 17 is based on the fact that bromide ions give rise to first-order quenching kinetics, i.e., during the fluorescence lifetime all probes experience an average bromide ion environment. In such a case the quenching rate is proportional to θ. By assuming that $[O_2]$ is constant, it follows from (17) that θ can be calculated from

$$\theta = \frac{\tau^{-1} - \tau_{\theta=0}^{-1}}{k_{Br}} \tag{18}$$

where $\tau_{\theta=0}$ is the lifetime at low β where θ is zero. In a previous study[7] k_{Br} was found to be 3.5×10^6 s^{-1} for CTAB micelles. In principle, k_{Br} may be affected by the presence of polyion, but we shall neglect that in the present analysis. The result calculated from the function fitted to the lifetime data shows that a substantial binding of bromide ions takes place for $\beta > 1$ (see Figure 14). Thus, the polyion is not the only counterion to the micelles in this range. In fact, by assuming that no simple salt enters the skins (see previous section), it follows from the electroneutrality condition that $\beta_{skin} = (1 - \theta)^{-1}$. We have included in Figure 14 the variation of β_{skin} with β obtained using

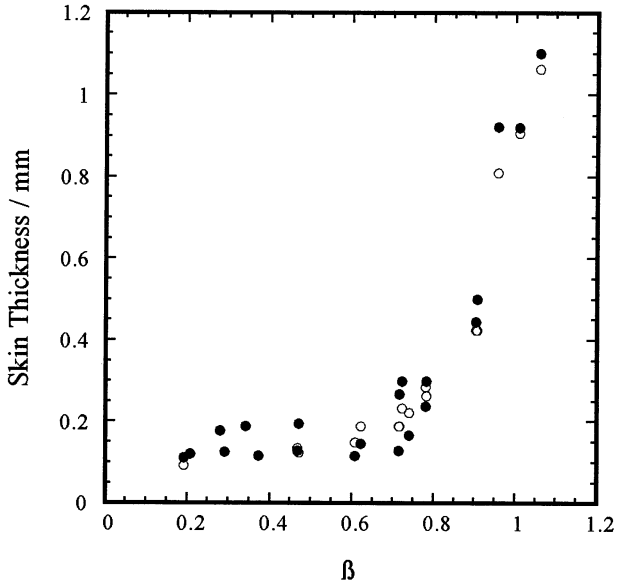

Figure 13. Thickness of skins on PA/CTAC gels (**III**) plotted vs β. Filled symbols: measured with micrometer; Open symbols: calculated from determined skin volumes and surface areas (see text).

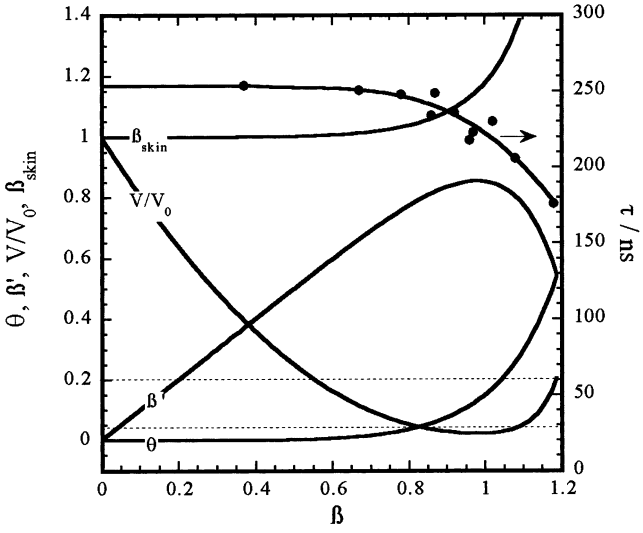

Figure 14. Fluorescence lifetimes (τ) of pyrene solubilized in PA/CTAB skins (**I**) plotted vs β (symbols), and a polynomial fit to the data (line). Other lines (see text): θ calculated from the fit using (18); $\beta_{skin}=(1-\theta)^{-1}$, $\beta' = \beta/\beta_{skin}$, $V/V_0 = (1-\beta')^2$.

this relationship. As can be seen, β_{skin} increases rapidly when β exceeds 0.8. However, it is smaller than 1.1 for a large range of β values, in agreement with the above estimate for PA/CTAC. It is interesting to note that the variation of β_{skin} implies that the fraction of the network taking part of the skin, i.e., β' ($=\beta/\beta_{skin}$), first increases with increasing β (as expected), goes through a maximum at $\beta \approx 1$, and then decreases, as indicated in Figure 14. It suggests that the core does not vanish completely. On the other hand, it should be heavily compressed (cf. Figure 8b) and therefore not immediately distinguishable from the skin. An interpretation is that polyion is gradually replaced by bromide ions as counterion to the micelle and "transferred" to the core. This is in agreement with the behavior of linear PA/CTAB complexes.[27] To appreciate such an effect on the gel volume we have calculated V/V_0 from β' using the parabolic approximation (14). The result is shown in Figure 14. The subject needs to be further investigated, however.

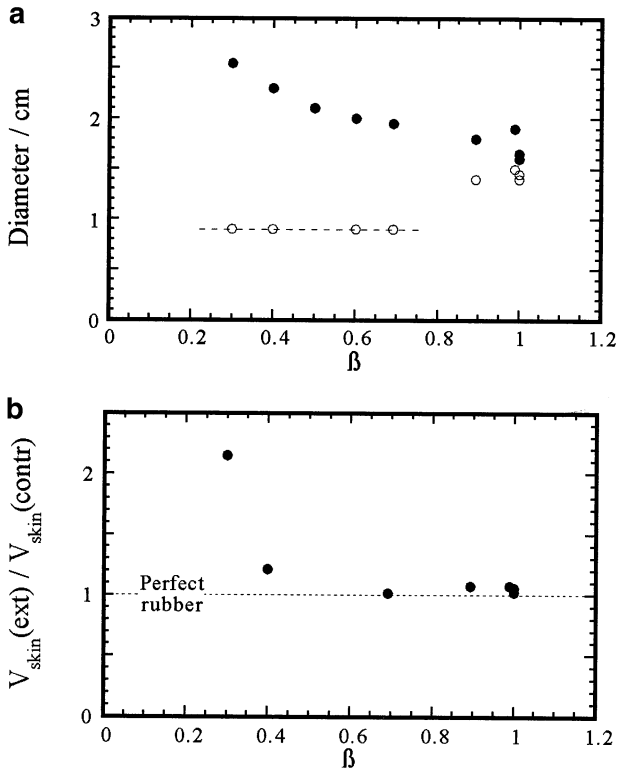

Figure 15. Elastic behavior of skins from PA/CTAB gels (**II**). (a) Diameter of intact gels (filled) and outer diameter of relaxed skins (open). Dashed line indicates the diameter of the test tubes in which the networks were synthesized. (b) Ratio of skin volume in extended and contracted states V_{skin}(ext)/V_{skin}(contr) plotted vs β. Indicated is the behavior of perfect rubber (dotted line).

Elasticity and Volume of Skin. The dissection described in Figure 3 was repeated for PA/CTAB gels (**II**) with different β. The gel specimens studied were the same as those used in Figure 9b. The contraction of skins (removed from the core) is evident from Figure 15a displaying the diameter of intact gels (filled symbols) and the outer diameter of relaxed skins, the latter measured after incubation in the solution for one month. Gels with $\beta > 0.6$ were of the "balloon" type mentioned above, i.e., with a liquid core. As can be seen these did not contract very much (except for $\beta = 0.7$), and the diameter in the relaxed state was larger than for gels with lower β. The reason for this is not clear but the phenomenon correlates with structural changes of the micelles (see next section).

For gels with lower β the outer diameter was reduced by a factor of 2 or more during contraction, revealing a large elasticity. Interestingly, the outer diameter in the contracted state was the same for all these gels and equal to the (inner) diameter of the test tubes the networks were synthesized in. It appears, thus, that the polymer network in the skins relaxed to a (presumably) isotropic state. The same was observed for fully collapsed gels formed under circumstances when balloon formation did not occur. The behavior is rather remarkable considering the high charge of the polymer chains. It suggests, however, that the interaction with the micelles, in this respect, is equivalent to that of neutralizing (i.e., protonating) the network charges.

Very intriguing is the observation mentioned in the Introduction that the skin volume did not change during contraction. This was observed for the present gels for $\beta > 0.4$, as can be seen in Figure 15b, where the ratio of skin volume in extended and contracted states is plotted vs β. Constant volume implies that the amount of water in the skins did not change during

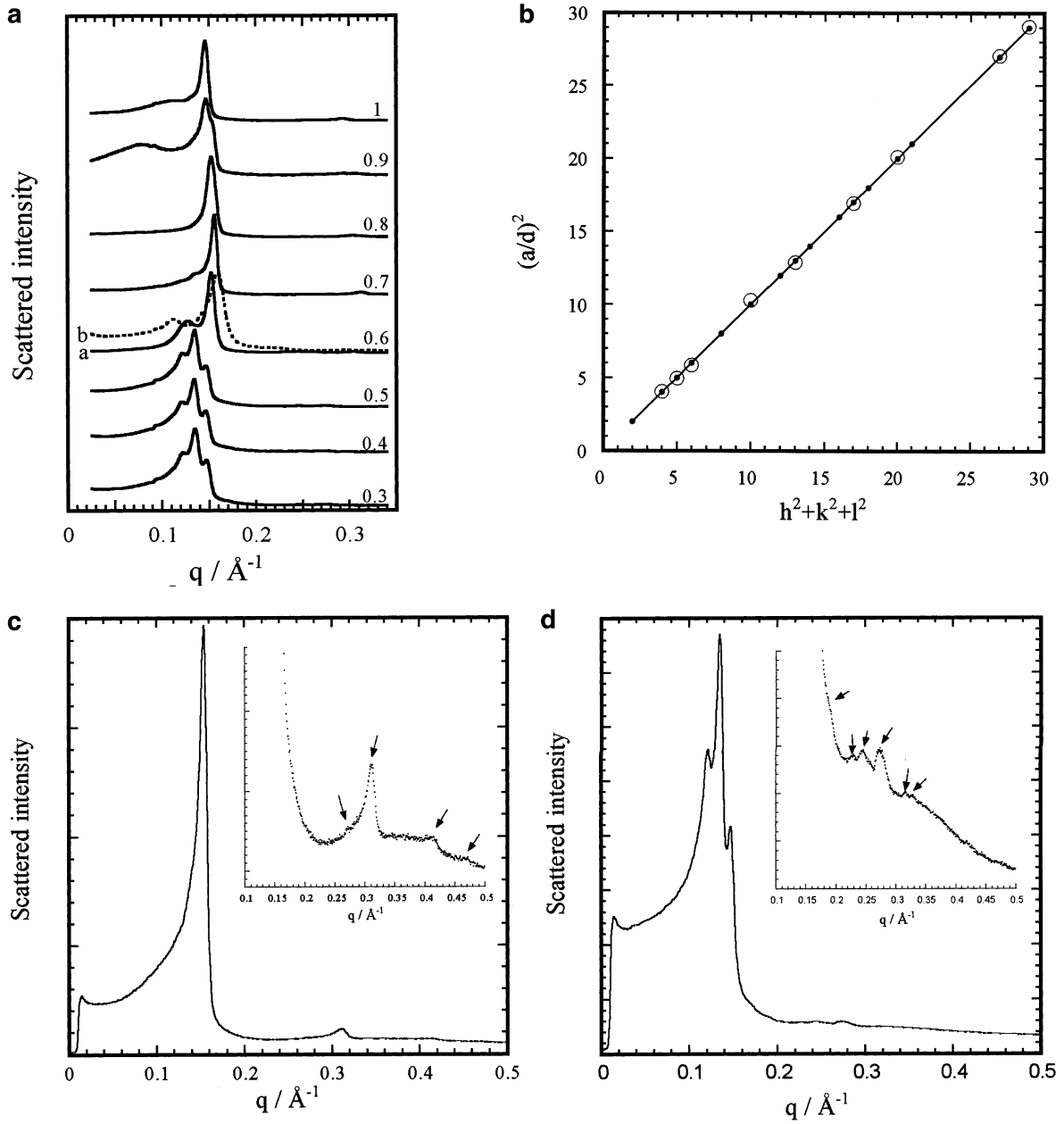

Figure 16. SAXS data from PA/CTAB skins. (a) Evolution of scattering profile with increasing β (indicated) for gels swelling in CTAB solution (**II**). (b) Theoretical (filled symbols) and observed (open symbols) values of $(a/d)^2$ as a function of $(h^2 + k^2 + l^2)$ for the cubic *Pm*3*n* space group. The latter were calculated from the lattice spacing and $a = 104.1$ Å, determined for the $\beta = 0.4$ sample in Figure 16a. (c) Scattering from skin with hexagonal structure from gel shrinking in 0.5 mM CTAB solution (**I**), $\beta = 0.9$. (d) Scattering from skin with cubic structure (*Pm*3*n*) from gel shrinking in 0.5 mM CTAB solution (**I**), $\beta = 0.9$.

contraction. Thus, no compositional change took place as the skins were deformed. At low β the water content decreased as the skins contracted, as shown by the volume ratio in Figure 15b. Conversely, the high water contents found in skins at low β can be interpreted as a swelling of the network upon stretching. It is interesting to note that polymer networks are known[44] to display either constant volume behavior (solvent-free rubber) or swelling (solvent swollen networks) upon stretching. Before discussing this further we shall consider the structure of the surfactant assemblies in the skins.

Skin Microstructure. The structure and organization of surfactant aggregates in PA/CTAB skins were investigated by means of SAXS and TRFQ. As a complement we also checked if the skins displayed optical birefringence.

SAXS profiles from skins taken from system **II** gels with different β are shown in Figure 16a. At low β reflections indicative of a cubic structure were found. The data fits to the primitive space group *Pm*3*n*,[46] as can be seen in Figure 16b where $(a/d)^2$ for the sample with $\beta = 0.4$ is plotted vs $(h^2 + k^2 + l^2)$, where a is the unit cell length, d is the lattice spacing $(=2\pi/q)$, and h,k,l are Miller indices. Filled symbols represent theoretical values for the *Pm*3*n* space group. Open symbols are experimental values calculated using a unit cell length of 104.1 Å. The same structure was found in a previous[33] study of PA/DoTAB gels, and has been reported also by others[47] for gels in the fully collapsed state.

At higher β the structure changes to hexagonal, with characteristic relative peak positions $1{:}\sqrt{3}{:}\ \sqrt{4}{:}\ \sqrt{7}$, etc. However, the lattice spacing increases with β, and some of the samples appear to contain more than one type of structure. The samples with $\beta = 0.8$ and $\beta = 1$ appear to be monophasic hexagonal with different lattice spacing, but the one with $\beta =$

0.9 appears to contain a mixture. For $\beta = 0.7$ the shoulder on the left-hand side of the main peak indicates that the skin may contain crystallites of a cubic structure in addition to the hexagonal domains. For the gel with $\beta = 0.6$ both the mantle (a) and the end parts (b) of the skin were examined. While the strong reflection in (a) has the same position as that for $\beta = 0.8$, the one in (b) is positioned at q even higher than that for $\beta = 0.7$. Both spectra contain several weak reflections at high q, indicating that there are cubic domains present, and in addition to that a broad peak at low q.

Most interestingly, however, is the coincidence between the transition from cubic to hexagonal structure and the appearance of the balloon phenomenon (observed for gels with $\beta > 0.6$). As pointed out in a preliminary report,[34] this correlation between changes on microscopic and macroscopic levels is found also for preswollen gels shrinking in CTAB solutions (**I**). Also in this case balloon gels (or liquid filled "blisters" on the gel surface) were observed exclusively at high β (>0.9) and displayed a hexagonal skin microstructure. A typical SAXS spectrum from such gels is shown in Figure 16c. However, not all system **I** gels with high β were of the balloon type, as evident from Figure 9a where V/V_0 for gels shrinking in a "regular" way is shown. SAXS measurements revealed that all these gels had a cubic structure of the type discussed above. In Figure 16d is given an example where the low q region has been enlarged. In a previous report[34] it was found that gels placed in 0.1 mM CTAB ($0 < \beta \leq 1$) all shrank in a regular fashion and had a cubic microstructure. No compositional analysis was made for these gels. However, it is likely that smaller amounts of bromide ions were incorporated in the skins as compared with gels placed in stronger CTAB solutions.

The unit cell of the *Pm*3*n* micellar cubic phase contains eight micelles: one positioned at each corner of the cube, one in the center, and two on each cube face.[48,49] This information permits the surfactant aggregation number (N) to be calculated. All skins from system **I** gels with cubic structure (and $\beta < 0.8$) were found to contain 46−48 wt % H_2O. Converting this to molar concentrations using (15) and using the estimated value of a (=104.5 Å) we obtain $N = 128$. Here we have used the relationship $N = C_{CTA}a^3N_A/8$, where N_A is Avogadro's number. The result shows that the micelles are globular but not spherical. By assuming a rod shape, and using group contributions to the surfactant tail volume[50] an axial ratio (length/diameter) of 1.3 is found, in perfect agreement with a value determined for micelles in the *Pm*3*n* micellar cubic phase of DoTAC/water.[51]

The radius r_{mic} of the hydrocarbon core of the micelles in the hexagonal phase and the distance b between them is given by following equations:

$$r_{mic} = d\sqrt{\frac{2\phi_{hc}}{\sqrt{3}\pi}} \tag{19}$$

$$b = \frac{2d}{\sqrt{3}} \tag{20}$$

where ϕ_{hc} is volume fraction of hydrocarbon core in the phase. For the hexagonal samples in Figure 16a, the micellar center-to-center distance thus calculated increases from 46 Å at $\beta = 0.7$−49 Å at $\beta = 1$, and at the same time the rod radius increases from 17 to 18 Å. As a result, the surface-surface distance between micelles changes very little. The increased lattice spacing observed as β increases from 0.7 to 1 is thus due to a thickening of the micelles, probably due, in turn, to an increased bromide ion binding.

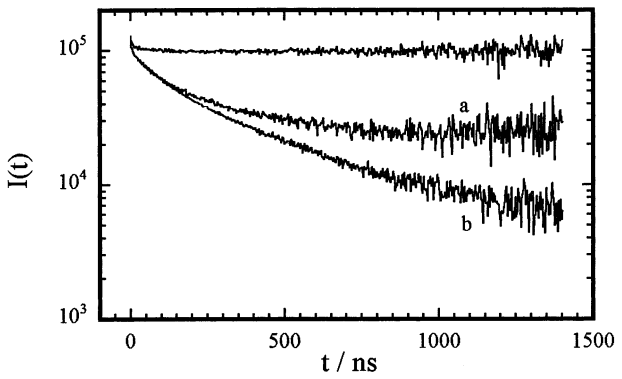

Figure 17. Normalized fluorescence decays from pyrene solubilized in skins of PA/CTAB gels (**I**) recorded in the absence (top curve) and in the presence of quencher CP^+. (a) Skin with cubic structure, $\beta = 0.4$. (b) Skin with hexagonal structure, $\beta = 1$.

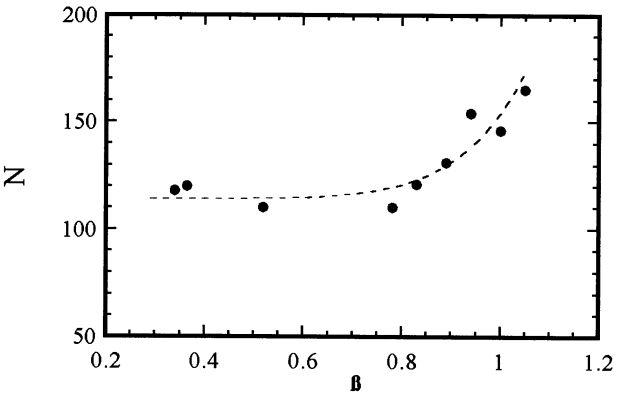

Figure 18. Surfactant aggregation numbers (N) in PA/CTAB gels (**I**) determined with TRFQ. All samples displayed cubic structure in SAXS experiments. The line is just a guide to the eye.

For system **I** the structural transition was also investigated with TRFQ, a technique which can be used to distinguish between closed and "infinite" surfactant assemblies. The result is clear: skins with cubic microstructure were found to contain small micelles, and skins with hexagonal ordering were found to contain large aggregates. Figure 17 shows examples of fluorescence decay curves from both types of skins, where in (a) the steady-state observed at long times, not present in (b), is characteristic of quenching in small micelles.[39] Please note that the decay curves have been multiplied by $\exp(t/\tau)$ to better display the two types of quenching kinetics. From curves of the type (a) the average aggregation number (N) can be obtained as described in the Experimental Section. The result for the present gels is shown in Figure 18, where N is given as a function of β. For $\beta \leq 0.8$, N is ca. 120, in good agreement with the estimate from SAXS measurements. The result proves that the cubic mesophase is made up from discrete micelles, and thus not bicontinuous as frequently observed in lipid systems.[52] Furthermore, the close agreement between the two estimates of N gives strong support to the proposed space group. At high β, N increases with β. This reflects the tendency of micelles to grow as bromide ions are incorporated in the complexes.

All skins were checked for birefringence by positioning them between crossed polarizers. Again the result was clear: skins with cubic structure were optically isotropic; those with hexagonal structure were anisotropic (birefringent). Of course, this is the result expected for liquid crystalline phases displaying these structures. However, one should keep in mind that an anisotropically deformed polymer network may also give rise to birefringence. Therefore, the nonbirefringence of skins with

cubic structure indicated that the network was deformed to the same extent in all directions parallel to the gel surface. (A test showed that the skins displayed strong birefringence when extended by force in the polarization direction of the light.) Skins that had relaxed after being removed from the swollen cores were also checked (system **II**). No change in optical birefringence was observed after contraction, proving that no transition from cubic to hexagonal structure took place.

We end this section by mentioning that, in contradiction to what has been reported by others,[53] we have never observed lamellar structures in fully collapsed gels or skins taken directly from wet gels. However, a PA/CTAB skin with hexagonal structure transformed into a lamellar structure upon drying.

Relation to Behavior of Linear PA/CTAB. Very recently Svensson et al.[28] studied the phase behavior of the "complex salt" CTAPA (free from Br^- and Na^+). By adding water to the pure salt a hexagonal phase was formed that could take-up approximately 49 w% water before transforming, via a very narrow two-phase region, into a cubic micellar phase (*Pm*3*n*) with a maximum water content of 56 w%. Upon further additions of water the cubic phase was in equilibrium with essentially pure water.

The spontaneous swelling of the hexagonal phase of pure CTAPA in water, and its conversion to the cubic phase, shows that the net interaction between the micelles is repulsive in that concentration range. It is thus likely that the structural transition is an effect of packing, resembling the transition from micellar cubic to hexagonal in the phase diagram of, e.g., CTAAc/water.[27] On the other hand, the limited swelling of the cubic phase shows that at higher water contents (i.e., larger separations between micelles) the net interactions become attractive. The attractions are most likely due to bridging and electrostatic correlations between "polyion-dressed micelles" (Figure 1). It is interesting that the structure in the cubic phase is the same as in the micellar cubic phase of CTAAc/water (and in the well studied system DoTAC/water[54]) where the net interaction is expected to be repulsive at all concentrations. However, the behavior is in agreement with results from statistical mechanics of fluids[55] showing that, no matter if the interaction potential is repulsive or attractive, the structure is mainly determined by short-range repulsive (steric) interactions.

The skins studied here may be viewed as cross-linked versions of the concentrated mesophases formed by CTAPA. The dense packing of complexes in them can therefore be explained by the presence of the same types of attractive interactions as in the case of linear PA. However, there is one additional factor that may affect the micelle structure in skins, namely, the anisotropic deformation of the network. As we have seen above the anisotropy is due to the presence of the swollen core, and varies with β. It appears, however, that the transition from cubic to hexagonal structure in the skins can be explained without resorting to such explanations. Support for this comes from the observation that the micelle structure was the same in extended and contracted skins. Instead the transition can be attributed to the binding of surfactant counterions. Svensson et al. found[28] that small amounts of CTAB could be incorporated into the cubic phase of linear CTAPA. However, in the presence of a dilute aqueous phase, the slightly more concentrated hexagonal phase started to appear already at 4 mol % of CTAB present (of the total amount of surfactant). Furthermore, when the amount of CTAB was larger than 20 mol % the cubic phase was completely replaced by the hexagonal phase coexisting with the dilute phase. In agreement with this, we have seen in system **I** that for medium range β-values, where the skins are essentially free from surfactant counterions, the cubic phase is in equilibrium with a swollen core network and a very dilute NaBr solution (containing trace amounts of CTAB). At higher β, surfactant counterions start to accumulate in the skins, which is followed by a growth of the micelles (see Figure 18). The hexagonal structure starts to appear at $\beta \approx 0.8$. We have indicated with dotted lines in Figure 14 the θ values corresponding to the phase boundaries in the phase diagram of Svensson et al.[28] Below $\theta = 0.04$ and above $\theta = 0.2$ monophasic cubic and hexagonal structures are expected, respectively. Between the lines the two structures should coexist. It is striking how well these limits coincide with the appearance of cubic and hexagonal structures in the skins. Indications of coexistence of the structures were observed in the SAXS spectra from system **II** skins (Figure 16a). The transition to hexagonal structure starts at a slightly lower β here than in system **I**, which is attributed to a larger bromide ion concentration in the system.

For the PA/CTAC gels (**III**) no SAXS measurements were made, but observations of optical birefringence indicated that the transition from cubic to hexagonal structure started at $\beta \approx 0.75$. Unfortunately, we have no information about surfactant counterion binding in this system, except from the estimates of β_{skin} (see above) indicating that $\theta \leq 0.08$ (here referring to chloride ions) for all β. However, in agreement with the behavior of non-crosslinked CTAPA complexes the transition between cubic and hexagonal took place at a water content of ca. 50 wt % (see Figure 12a). Interestingly, the birefingence was markedly enhanced for samples with $\beta > 1$, suggesting that these were monophasic hexagonal, and that samples in the range $0.75 < \beta < 1$, showing weaker birefringence, contained a mixture of cubic and hexagonal structures. These observations are, again, in agreement with what can be expected from the behavior of non-cross-linked CTAPA.

We do not know the extension of the cubic phase toward low β but for PA/CTAB (**II**) SAXS measurements confirmed that the cubic structure was present at $\beta = 0.3$ (57 wt % water). The substantial amount of water in the skins observed at low β for PA/CTAC (**III**) makes long-range structural order unlikely. For comparison, in systems with long-range repulsive interactions, such as CTAAc/water (Ac = acetate ion), the addition of water leads to a transition from cubic to disordered micellar phase at 70−80 wt % water.[27] In fact, we have recently observed dissordered micellar structures in PA/DoTAB skins with $\beta = 0.2$.[56] It is not clear how these observations relate to the limited swelling of the cubic phase in non-cross-linked CTAPA. Possibly, there is an effect of the network deformation. Order−dissorder transitions have been observed by Ashbaugh et al.[57] following swelling caused by the incorporation of nonionic surfactants in fully collapsed PA/DoTAB gels.

Structural Basis for Rubber Elasticity. Solvent-free rubber can be deformed without any change in volume. The reason for this is that the deformation occurs without a change of the average contact distance between polymer chain segments in the sample.[43] Thus, there is no enthalpy change, rather the elasticity is due to the reduction of the configurational entropy of the network chains upon deformation of the rubber.

As demonstrated above, some of the skins studied display rubber-like behavior. In the skins the swelling of the network is controlled by the polyion/micelle interaction. Deformation at constant volume requires the interaction not to change. How is it possible to deform the skin without changing the polyion/micelle interaction? First of all, at constant volume a lateral stretching of the network is followed by compression in the direction perpendicular to the gel surface. Thus, there is no

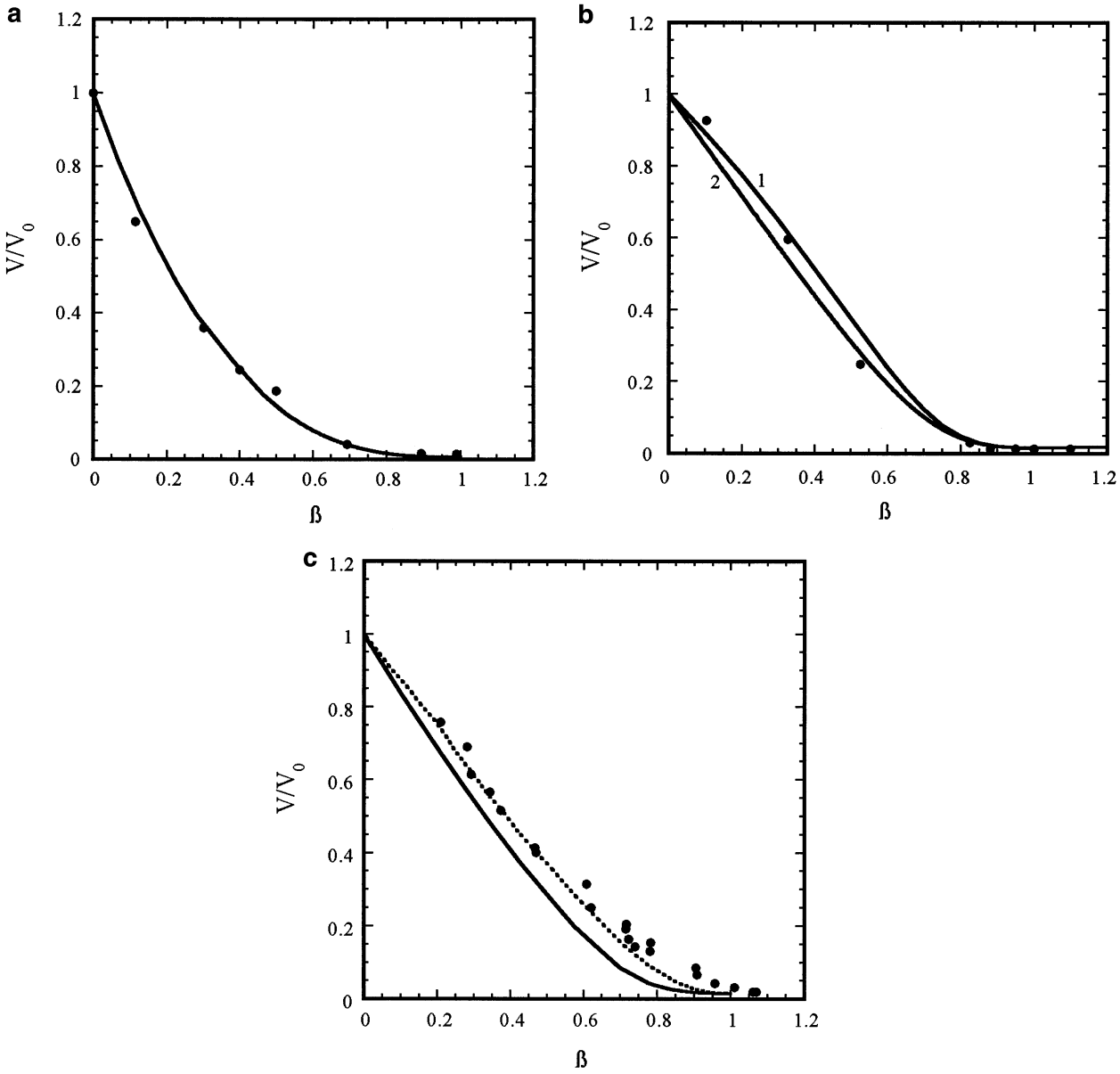

Figure 19. Comparison between model calculations (lines) and experiments (symbols) for PA gels. V/V_0 is given as a function of β. Theoretical curves were obtained with $k_4 - k_6$ for 1% X in Table 2, and $p = 50$. (a) Swelling in CTAB solutions (**II**). Theoretical curve: $\upsilon_{skin} = 3 \times 10^{-4}$ m^3/mol. (b) Shrinking in 0.5 mM CTAB solutions (**I**). Theoretical curves: (1) v_{skin} = line in Figure 12b, (2) $\upsilon_{skin} = 7 \times 10^{-4}$ m^3/mol. (c) Shrinking in CTAC solutions. Theoretical curves: υ_{skin} = line in Figure 12b. Dashed line: $p = 115$.

change in the average concentration of polyion in the skins. Second, since the micelles occupy a large fraction of the volume in the skin the concentration of polyion units is very high in the aqueous region between them (ca. 3 M). Thus, even in the stretched out skins an effective charge compensation may be accomplished; the stretching inevitably leads to breaking of micelle-polyion "bonds", but is followed by the recreation of equivalent ones. However, the deformations reduce the configurational freedom of the network chains, which leads to a reduction of entropy. We believe this is the reason for the rubber-like behavior of the skins.

Interestingly, the transition from cubic to hexagonal structure affects the elastic behavior of the skins, and seems to be responsible for the appearance of liquid filled gels, so-called "balloons". A full understanding of the latter phenomenon requires detailed studies of the dynamics of skin formation. However, as inferred from Figure 15a, balloons form when the lateral contraction of the skin is prohibited or is extremely slow. In this case, as the collapse of the core network proceeds, the gels maintain a large outer radius. During this stage the conversion of core network into skin at the interface between the two phases leads to a partial destruction of the network. One explanation may be that the hexagonal microstructure, which is intrinsically anisotropic, favors an anisotropic state of the polyion network consistent with a lateral extension of the skin.

Comparison Between Theory and Experiments. The V/V_0 curves shown in the theoretical part of the paper are in qualitative agreement with swelling experiments.[34,38,58−61] However, the conditions were idealized to better demonstrate the sensitivity of the model to different parameters. In this section we try to mimic the situations in real experiments to make a quantitative test of the model.

Figure 19a shows the result for the case when initially dry PA gels swell in CTAB solutions (**II**). For balloon gels ($\beta \geq 0.7$), the volume of the enclosed liquid has been subtracted. To obtain the theoretical curve V/V_0 was calculated as a function of β for given values of υ_{skin} and p, using (5) and (10−13).

Here we put $\beta = \beta'$, with support from the compositional analysis showing that $\beta_{skin} \approx 1$. The value of the constants k_4-k_6 in (13) were taken from Table 2 (1% X). However, since the total amount of CTAB in the system was varied at fixed amount of PA gel, the electrolyte concentration in the solution was not constant. To account for this in the model the constants k_1-k_3 describing $\Delta\pi_{ion}$ in (12) was determined for each electrolyte concentration, as described in the Appendix. υ_{core} was then solved for numerically, and used in (5) to calculate V/V_0. To obtain the calculated curve the procedure was repeated for a number of β in the range from zero to unity. Note that all β correspond to different electrolyte concentrations in the solution. As can be seen in Figure 19a the model curve fits well to the experimental data. The curve was obtained with $p = 50$ and $\upsilon_{skin} = 3 \times 10^{-4}$ m^3/mol. Since p is the average length of polymer chains in the network, determined by the degree of cross-linking (1%), υ_{skin} is the only adjustable parameter. It is slightly lower than determined experimentally for PA/CTAC (Figure 12b), but of the correct order of magnitude. The significance of this will be discussed at the end of the paragraph; for the dependence of V/V_0 on υ_{skin} in the model, see Figure 8c.

According to experiments the water content in the PA/CTAB (**II**) skins decreased from 57 to ca. 40 wt % as β changed from 0.3 to unity. This rather moderate variation motivates the use of a constant value of υ_{skin} in the calculations. However, an error may be introduced at low β where the water content is considerably larger; see Figure 12b. In Figure 19b we have taken care of this effect by letting υ_{skin} depend on β as indicated by the dashed line in Figure 12b. The constants k_1-k_6 and p were chosen to match the conditions of system **I**. Again the result (curve 1) is in good agreement with experiments. Note that the ionic strength in the solution is fixed in this case. Shown is also the result from a calculation with $\upsilon_{skin} = 7 \times 10^{-4}$ m^3/mol for all β (curve 2). A comparison between the two calculated curves shows that the effect of varying υ_{skin} is distinct but small. This is expected since at low β, where υ_{skin} changes most, the skin has the smallest influence on the core.

As a last example we have calculated υ_{core} and V/V_0 as functions of β with input parameters corresponding to PA/CTAC (system **III**), where again the ionic strength in the solution varies. Here we have used as input parameters $p = 50$ and the experimentally determined υ_{skin} values in Figure 12b. The results are shown in Figures 11 and 19c, respectively. As can be seen the agreement with experiments is not perfect, but reasonable considering that the curves are obtained without any fitting parameters. By keeping in mind that the theory behind (8) involves a number of approximations the agreement is not expected to be better. In fact, the result from more rigorous theories of rubber elasticity shows that n in (8) should be replaced by λn, where λ is a material constant taking care of network defects among other things.[43] Results from attempts to determine λ from experiments on rubber show that it does not deviate too much from unity.[43] By taking over these results to the present systems, it means that p in (10) should be multiplied by a correction factor of order unity. The dotted line in Figure 19c represents the result of using a correction factor of 2.3. Since the product $p\upsilon_{skin}^{2/3}$ occurs in the denominator of (10), this correction is equivalent to treating υ_{skin} as a fitting parameter, and p as determined by the degree of cross linking, as we did above. It is encouraging, therefore, that υ_{skin} obtained in this way agrees with experiments to within the correct order of magnitude.

Conclusions

Polyion/surfactant complexes form a separate 'surface phase' in the gel distinct from the swollen gel core. The complexes consist of closely packed surfactant micelles with polyion chains in the aqueous regions between them. The driving force behind the phase separation is the same as for linear PA/CTAB/water. Similar to what has been observed in the latter type of systems, the size of micelles, their shape, and spatial organization are affected by the amounts of polyion and simple ions in the skins. Thus, when the charge ratio between micelle and polyion in skin is close to unity a micellar cubic phase is formed. However, when the surfactant is in sufficiently large excess, so that bromide (or chloride) ions are incorporated in the complexes, a hexagonal phase of rodlike micelles is formed.

An important difference between skins and concentrated phases of linear PA/CTAB is the elasticity of the former due to the cross-links. In particular, skins with cubic microstructure have rubber-like properties. However, the position of the skin outside the swollen core implies that the deformation of the skin network is nonuniform. The lateral average extension of the network chains is by necessity about the same as in the core (exactly the same at the core/skin boundary), but in directions normal to the gel surface the network is compressed. This has two important consequences: First, the skin exerts a pressure on the core, reducing its degree of swelling. Second, the extent of deformation of the skin network depends on the swelling of the core, and so does, in principle, the polyion/micelle interactions in the skin. In particular, since υ_{core} is a function of β, the anisotropy of the skin network is a function of β. This variable, not present in systems of linear polyion/surfactant, may affect the composition of the skins, e.g., their water content and microstructure. To what extent the network deformation influences the skins studied in this work is not completely clarified, but it may be responsible for the high water content in skins at low β. This could in turn explain the absence of crystalline structures observed in skins from PA/DoTAB gels at low β.[56]

The essential characteristics of equilibrium swelling curves observed in gel/surfactant systems can be accounted for theoretically by considering the rubber elasticity of the skins. In the present work we have calculated explicitly the work of deforming the skin network and used the Laplace equation to calculate the pressure exerted on the gel core. While introducing some approximations, e.g., curvature effects are neglected; it provides a conceptually clear description of swelling equilibrium in phase-separated gels.

Acknowledgment. We are grateful to Mr. Göran Dahl for skilfull technical assistance. This work was financially supported by Center for Amphiphilic Polymers (CAP), Lund University, and the Swedish Research Council.

Appendix

Poisson−Boltzmann(PB)Cell Model.[62] The polyion is described as an infinitely long cylinder of radius r_0 with a uniform surface charge density equal to $e/(2\pi r_0 l)$, where e is the electronic charge and l is the separation between charged groups along the (real) polyion chain. The charged cylinder is positioned at the center of a cylindrical cell of radius r_{cell} containing water and mobile ions. The distribution of mobile ions in the cell is

obtained from a solution of the PB-equation, which in cylindrical coordinates becomes

$$\frac{1}{r}\frac{\mathrm{d}}{\mathrm{d}r}\left(r\frac{\mathrm{d}\psi}{\mathrm{d}r}\right) = -\frac{F}{\epsilon_0\epsilon_\mathrm{r}}\sum_\mathrm{i} z_i C_i \exp(-z_i F\psi/\mathrm{R}T) \quad r_0 < r \le r_\mathrm{cell} \tag{A:1}$$

where ψ(r) is the mean electrostatic potential, F the Faraday constant, ϵ_0 the permittivity of vacuum, ϵ_r the relative permittivity, z_i the valence of ion i, and C_i its concentration in a polyion-free solution in equilibrium with the cell, where ψ is defined to be zero. Equation A:1 can be solved[63] with the boundary conditions $(\mathrm{d}\psi/\mathrm{d}r)_{r=r_0} = -\sigma/\epsilon_0\epsilon_r$ and $(\mathrm{d}\psi/\mathrm{d}r)_{r=r_\mathrm{cell}} = 0$. When salt is present it must be solved numerically. In the present paper we used a computer program written by Bengt Jönsson.[64]

The PB-equation is based on the assumption of a Boltzmann distribution of the ions in an effective potential ψ, which implies that the correlation between small ions is neglected. Furthermore the charged interface is assumed to be smooth with a uniform surface charge density, and the solvent is treated as a dielectric continuum. Despite these simplifications the errors introduced are not too serious for the calculations of thermodynamic quantities in the case of monovalent counterions.[65]

Calculation of $\Delta\pi_\mathrm{ion}$. The PB-cell model was used to calculate the distribution of salt between solution and gel core at a given degree of swelling. The cell was defined by $r_0 = 2$ Å, $l = 2.5$ Å, and $r_\mathrm{cell} = (\upsilon_\mathrm{core}/\pi l)^{1/2}$. The following procedure was used to calculate the equilibrium distribution of ions in a system containing a specified amount of of 1:1-electrolyte: (1) The PB-equation was solved for a chosen activity of salt (=concentration of salt in the solution), and the result was used to calculate the mean concentration of salt in the cell by integration of the obtained ion concentration profiles. (2) The total amount of salt in the system (gel + solution) was calculated using the result in step 1 and the volume of gel and solution. (3) Steps 1 and 2 were repeated with a new salt activity until the amount of salt in the system was equal to the specified value.

In the PB-cell model the activity of a mobile ion i is equal to its concentration at the cell border $C_i(r_\mathrm{cell})$, and the osmotic pressure is[66]

$$\pi_\mathrm{ion} = RT\sum_\mathrm{i} C_i(r_\mathrm{cell}) \tag{A:2}$$

$\Delta\pi_\mathrm{ion}$ was calculated from the relationship

$$\Delta\pi_\mathrm{ion} = RT\sum_i C_i(r_\mathrm{cell}) - 2RTC_\mathrm{salt} \tag{A:3}$$

obtained from (A:2) and by neglecting ionic interactions in the solution. To find a relationship between $\Delta\pi_\mathrm{ion}$ and υ_core for a given amount of electrolyte, we calculated $\Delta\pi_\mathrm{ion}$ for a series of υ_core values, and fitted (12) to the data plotted in a graph. This gave the value of the parameters k_1-k_3. The procedure was repeated for all electrolyte concentrations of interest.

Nomenclature

List of Symbols

β: number of surfactants per polyion unit in gel
β': fraction in skin of total amount of polyion units
β_skin: molar ratio of surfactant to polyion in skin
$C_\mathrm{s,sln}$: concentration of surfactant in solution
$C_\mathrm{s,tot}$: total surfactant concentration
$C_\mathrm{p,tot}$: total concentration of polyelectrolyte monomers
$I(t)$: fluorescence intensity at time t
τ: fluorescence lifetime
$\langle n\rangle$: average number of quencher per micelle
k_q: intramicellar quenching rate constant
N: surfactant aggregation number
X_i: mole fraction of i in mixed micelles
n_p: number of moles of polymer units in gel
n_s: number of moles of surfactant in gel (skin)
υ_core: volume of core per moles of polymer units
υ_skin: volume of skin per moles of polymer units
V: gel volume
V_core: core volume
V_skin: skin volume
V_0: gel volume in surfactant free system
υ_0: gel volume per moles of polymer units in surfactant free system
π: osmotic pressure
π_skin: contribution to osmotic pressure from skin elasticity
π_ion: contribution to osmotic pressure from mobile ions
π_net: contribution to osmotic pressure from core network elasticity
γ: work (per unit area) of increasing skin surface area
R: core radius (spherical gel)
A: surface area of rubber sheet (skin)
A_ref: surface area of rubber sheet (skin) in nondeformed state
n: number of moles of polymer chains in rubber sheet (skin)
R ideal gas constant
T absolute temperature
p average number of polymer units between cross-links
k_1-k_6: parameters used to describe π_ion and π_net as functions of υ_core
M_app: apparent molar mass of surfactant/polyion complexes
m: gel mass
m_skin: skin mass
n_Na: number of moles of Na^+ in skin
n_CTA: number of moles of CTA^+ in skin
k_0: natural decay rate of excited fluorescent probe
k_ox: first-order rate constant for quenching with oxygen
$[O_2]$: concentration of oxygen in water
k_Br: rate constant for quenching with bromide ions
θ: number of bound bromide ions per surfactant in micelle
$\tau_{\theta=0}$ fluorescence lifetime at zero θ
q: scattering vector
h,k,l: Miller indices
d: lattice spacing
a: cubic structure unit cell length
r_mic: hydrocarbon core radius of micelle in hexagonal phase
b: distance between micelles in hexagonal phase
ϕ_hc: hydrocarbon core volume fraction in hexagonal phase
λ: network material constant
e: charge of electron
l: distance between charged groups on polyion
r_0: radius of charged cylinder in PB-cell model
r_cell: cell radius
ψ: electrostatic potential
F: Faraday constant
ϵ_0: permittivity of vacuum
ϵ_r: relative permittivity
z_i: valence of ion i
C_i: concentration of i in solution

C_{salt}: total concentration of 1:1-electrolyte in solution
$C_i(r_{cell})$: concentration of i at cell border

References and Notes

(1) Shirahama, K.; Yuasa, H.; Sugimoto, S. *Bull. Chem. Soc. Jpn.* **1981**, *54*, 375.
(2) Hayakawa, K.; Kwak, J. C. T. *J. Phys. Chem.* **1982**, *86*, 3866.
(3) Hayakawa, K.; Santerre, J. P.; Kwak, J. C. T. *Macromolecules* **1983**, *16*, 1642.
(4) Abuin, E. B.; Scaiano, J. C. *J. Am. Chem. Soc.* **1984**, *106*, 6274.
(5) Chu, D.; Thomas, J. K. *J. Am. Chem. Soc.* **1986**, *108*, 6270.
(6) Skerjanc, J.; Kogej, K.; Vesnaver, G. *J. Phys. Chem.* **1988**, *92*, 6382.
(7) Almgren, M.; Hansson, P.; Mukhtar, E.; van Stam, J. *Langmuir* **1992**, *8*, 2405.
(8) Kiefer, J. J.; Somasundaran, P.; Ananthapadmanabhan, K. P. *Langmuir* **1993**, *9*, 1187.
(9) Hansson, P.; Almgren, M. *Langmuir* **1994**, *10*, 2115.
(10) Hansson, P.; Almgren, M. *J. Phys. Chem.* **1995**, *99*, 16694.
(11) Hansson, P.; Almgren, M. *J. Phys. Chem.* **1996**, *100*, 9038.
(12) Hansson, P.; Almgren, M. *J. Phys. Chem.* **1995**, *99*, 16684.
(13) Hansson, P. *Langmuir* **2001**, *17*, 4161.
(14) Thalberg, K.; Lindman, B.; Karlström, G. *J. Phys. Chem.* **1990**, *94*, 4289.
(15) Hansson, P. *Langmuir* **2001**, *17*, 4167.
(16) Wallin, T.; Linse, P. *Langmuir* **1996**, *12*, 305.
(17) Wallin, T.; Linse, P. *J. Phys. Chem.* **1996**, *100*, 17873.
(18) Wallin, T.; Linse, P. *J. Phys. Chem.* **1997**, *101*, 5506.
(19) Haronska, P.; Vilgis, T. A.; Grottenmüller, R.; Schmidt, M. *Macromol. Theory Simul.* **1998**, *7*, 241.
(20) Kuhn, P. S.; Levin, Y.; Barbosa, M. C. *Chem. Phys. Lett.* **1998**, *298*, 51.
(21) Netz, R. R.; Joanny, J.-F. *Macromolecules* **1999**, *32*, 9026.
(22) Mateescu, E. M.; Jeppesen, C.; Pincus, P. *Europhys. Lett.* **1999**, *46*, 493.
(23) Gurovitch, E.; Sens, P. *Phys. Rev. Lett.* **1999**, *82*, 339.
(24) Park, S. Y.; Bruinsma, R. F.; Gelbart, W. M. *Europhys. Lett.* **1999**, *46*, 454.
(25) Granfeldt, M. K.; Jönsson, B.; Woodward, C. E. *J. Phys. Chem.* **1991**, *95*, 4819.
(26) Ilekti, P.; Piculell, L.; Tournilhac, F.; Cabane, B. *J. Phys. Chem. B* **1998**, *102*, 344.
(27) Ilekti, P.; Martin, T.; Cabane, B.; Piculell, L. *J. Phys. Chem. B* **1999**, *103*, 9831.
(28) Svensson, A.; Piculell, L.; Cabane, B.; Ilekti, P. *J. Phys. Chem. B* **2002**, *106*, 1013.
(29) Thalberg, K.; Lindman, B.; Karlström, G. *J. Phys. Chem.* **1991**, *95*, 6004.
(30) Thalberg, K.; Lindman, B.; Bergfeldt, K. *Langmuir* **1991**, *7*, 2893.
(31) Thalberg, K.; Lindman, B. *Langmuir* **1991**, *7*, 277.
(32) Khandurina, Y. V.; Rogacheva, V. B.; Zezin, A. B.; Kabanov, V. A. *Polym. Sci.* **1994**, *36*, 184.
(33) Hansson, P. *Langmuir* **1998**, *14*, 4059.
(34) Hansson, P.; Schneider, S.; Lindman, B. *Prog. Colloid Polym. Sci.* **2000**, *115*, 342.
(35) Karabanova, V. B.; Rogacheva, V. B.; Zezin, A. B.; Kabanov, V. A. *Polym. Sci.* **1995**, *37*, 1138.
(36) Zezin, A. B.; Rogacheva, V. B.; Kabanov, V. A. *Macromol. Symp.* **1997**, *126*, 123.
(37) Panyukov, S.; Rabin, Y. *Macromolecules* **1996**, *29*, 8530.
(38) Hansson, P. *Langmuir* **1998**, *14*, 2269.
(39) Almgren, M. *Adv. Colloid Interface Sci* **1992**, *41*, 9.
(40) Infelta, P. P.; Grätzel, M.; Thomas, J. K. *J. Phys. Chem.* **1974**, *78*, 190.
(41) Tachiya, M. *Chem. Phys. Lett.* **1975**, *33*, 289.
(42) Tomari, T.; Doi, M. *Macromolecules* **1995**, *28*, 8334.
(43) Treloar, L. R. G. *The Physics of Rubber Elasticity*; Oxford University Press: Oxford, 1958.
(44) Hill, T. L. *An Introduction to Statistical Thermodynamics*, 2nd ed.; Addison-Wesley Publishing Co.: Reading, MA, 1962.
(45) Tanford, C. *Physical Chemistry of Macromolecules*; John Wiley & Sons: New York, 1961.
(46) *International Tables for X-ray Crystallography*; Kynoch Press: Birmingham, U.K., 1952.
(47) Zhou, S.; Burger, C.; Yeh, F.; Chu, B. *Macromolecules* **1998**, *31*, 8157.
(48) Fontell, K.; Fox, K. K.; Hansson, E. *Mol. Cryst. Liq. Cryst.* **1985**, *1*, 9.
(49) Vargas, R.; Mariani, P.; Gulik, A.; Luzzati, V. *J. Mol. Biol.* **1992**, *225*, 137.
(50) Tanford, C. *The Hydrophobic Effect*: *Formation of Micelles and Biological Membranes*, 2nd ed.; John Wiley & Sons: New York, 1980.
(51) Johansson, L. B.-Å.; Söderman, O. *J. Phys. Chem.* **1987**, *91*, 5275.
(52) Fontell, K. *Adv. Colloid Interface Sci.* **1992**, *41*, 127.
(53) Khandurina, Y. V.; Dembo, A. T.; Rogacheva, V. B.; Zezin, A. B.; Kabanov, V. A. *Polym. Sci.* **1994**, *36*, 189.
(54) Balmbra, R. R.; Clunie, J. S.; Goodman, J. F. *Nature* **1969**, *222*, 1159.
(55) McQuarrie, D. A. *Statistical Mechanics*; Harper & Row: New York, 1976.
(56) Hansson, P. To be published.
(57) Ashbaugh, H. S.; Lindman, B. *Macromolecules* **2001**, *34*, 1522.
(58) Khokhlov, A. R.; Kramarenko, E. Y.; Makhaeva, E. E.; Starodubtzev, S. G. *Macromolecules* **1992**, *25*, 4779.
(59) Sasaki, S.; Fujimoto, D.; Maeda, H. *Polymer Gels Networks* **1995**, *3*, 145.
(60) Sasaki, S.; Yamazoe, Y.; Maeda, H. *Langmuir* **1997**, *13*, 6135.
(61) Ashbaugh, H. S.; Piculell, L.; Lindman, B. *Langmuir* **2000**, *16*, 2529.
(62) Fuoss, R. M.; Katchalsky, A.; Lifson, S. *Proc. Natl. Acad. Sci. U. S. A.* **1951**, *37*, 579.
(63) Gunnarsson, G.; Jönsson, B.; Wennerström, H. *J. Phys. Chem.* **1980**, *84*, 3114.
(64) Computer program written by Bengt Jönsson available at http://www.membfound.lth.se/chemeng1/prog.html.
(65) Jönsson, B.; Wennerström, H.; Halle, B. *J. Phys. Chem.* **1980**, *84*, 2179.
(66) Marcus, R. *J. Chem. Phys.* **1955**, *23*, 1057.